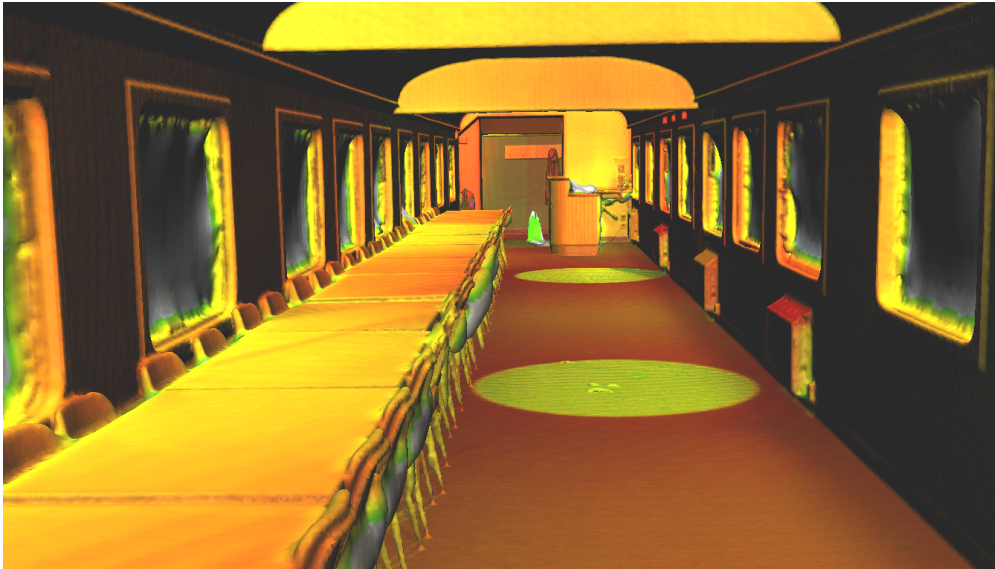




CHALMERS
UNIVERSITY OF TECHNOLOGY



The technical feasibility of providing passenger Wi-Fi with 60 GHz WiGig networks on board trains

Master's thesis in Communication Engineering

RIKARD REINHAGEN

MASTER'S THESIS EX074/2018

**The technical feasibility of providing passenger
Wi-Fi with 60 GHz WiGig networks on board
trains**

RIKARD REINHAGEN



CHALMERS
UNIVERSITY OF TECHNOLOGY

Department of Electrical Engineering
Division of Communication and Antenna systems
CHALMERS UNIVERSITY OF TECHNOLOGY
Gothenburg, Sweden 2018

The technical feasibility of providing passenger Wi-Fi with 60 GHz WiGig networks
on board trains

RIKARD REINHAGEN

© RIKARD REINHAGEN, 2018.

Supervisors: Mats Karlsson, Icomera AB
Claes Beckmann, KTH Royal Institute of Technology
Yasaman Ettefagh, Department of Electrical Engineering, Chalmers University of
Technology

Examiner: Erik Ström, Department of Electrical Engineering, Chalmers University
of Technology

Master's Thesis EX074/2018
Department of Electrical Engineering
Division of Communication and Antenna systems
Chalmers University of Technology
SE-412 96 Gothenburg
Telephone +46 31 772 1000

Cover: Mesh 3D file based on LIDAR measurements

Gothenburg, Sweden 2018

The technical feasibility of providing passenger Wi-Fi with 60 GHz WiGig networks on board trains

RIKARD REINHAGEN

Department of Electrical Engineering
Chalmers University of Technology

Abstract

To satisfy the usage of high data rate services such as 4K video streaming, Virtual Reality (VR) and Augmented Reality (AR) on board trains, new approaches are required. Current on board solutions cannot support these services for very crowded train carriages, due to the limited available spectrum in the currently used 2.4 and 5 GHz bands. One approach to this problem is to complement current Wi-Fi installations with new 60 GHz WLAN ("WiGig") radios, based on standards such as IEEE 802.11ad and 802.11ay. Currently these technologies are not extensively deployed for user devices, and the use case of 60 GHz access points inside train carriages is unexplored.

In this thesis, the technical feasibility, with focus on channel characteristics, physical and regulatory limitations, of 60 GHz communication systems using 802.11ad for passenger WLAN on board trains is evaluated. Three main investigation methods are used to evaluate this, a measurement campaign, analytical simulations and ray tracing simulations. The measurement campaign is performed at a train carriage in Gothenburg, Sweden. The TCP throughput and signal strength are mapped for the train carriage with a high accuracy indoor positioning system. The 60 GHz radio channel inside the train carriage is characterized by path loss exponent and fading standard deviation. The path loss exponent was found to be 1.5, which means that there is less signal degradation compared to free space loss. The measurement results show that, for this measurement setup, the use of 802.11ad-based communication systems for passenger WLAN on board trains can provide gigabit capacity and sufficient coverage with one to two access points per carriage. A LIDAR scanner was used to create a 3D model of the interior of the train carriage. The generated 3D model was used to run ray tracing simulations, which shows similar propagation characteristics as the measurements. A system level capacity study comparing a 5 GHz and a 60 GHz WLAN system is performed. The results show an order of magnitude higher capacity for the 60 GHz system under current spectrum regulations in the ETSI region for indoor usage.

A system level capacity study considering two 802.11ad-based access points inside a train carriage is performed. The results show a significant reduction ($\sim 70\%$) in capacity when the same channel is used within a train carriage compared to the interference free case. Adjacent channel usage shows a degradation ($\sim 25\%$) in capacity. By using sparsely spaced channels, only a reduction of $\sim 2\%$ in capacity is predicted compared to the interference free case.

Keywords: mmWave, millimeter wave, trains, 802.11ad, 802.11ay, 60GHz, WLAN, LIDAR

Acknowledgements

I have a lot of people to thank, for both giving me the opportunity to perform this thesis and for all the advise and support they have provided. I would like to start to thank Mats Karlsson at Icomera for giving me the freedom to form the direction of the thesis and choose one that interests me, whilst still being able to contribute with useful results to Icomera. A big thanks to Professor Claes Beckman from KTH who has helped to find a suitable scientific direction for this work, and helped to guide me during the execution of the project. Then I would like to thank my examiner Professor Erik Ström for providing the opportunity to perform this thesis, and for taking the time and interest to discuss the direction of the work. I would also like to thank Peter Eklund and Joel Bjurström at Icomera for all the feedback, ideas and discussion related to the project. I would also like to thank Maja Barring, from the Department of Industrial and Materials Science at Chalmers, for helping with the 3D scanning of the train carriage. Then I would like to thank my advisor Yasaman Ettefagh for being very helpful with providing advise and feedback related to the thesis.

Rikard Reinhagen, Gothenburg, May 2018

Contents

List of Figures	xiii
List of Tables	xv
List of Abbreviations	xvii
1 Introduction	1
1.1 Motivation for millimeter waves on trains	2
1.2 Challenges of millimeter wave communications	3
1.3 Scope	3
1.4 Thesis Aim and Contribution	4
1.5 Previous work	4
2 Theoretical background	7
2.1 Millimeter wave communications	7
2.2 60 GHz wave propagation	8
2.3 IEEE millimeter wave standards	9
2.3.1 802.11ad	9
2.3.2 802.11ay	10
2.3.3 WLAN channels	10
2.3.4 Transmit mask	11
2.3.5 Channel access method	11
2.3.6 Fast Session Transfer	12
2.4 Spectrum regulations	12
2.4.1 European region (ETSI)	12
2.4.2 USA (FCC)	12
2.5 Wireless channel modeling	13
2.6 Capacity calculation	14
2.7 Radio channel characterization	16
3 Methods	19
3.1 System level simulation	20
3.1.1 Capacity simulation	20
3.1.2 System model for interference investigation	21
3.2 Measurements	23
3.2.1 Measurement campaign	23
3.2.2 60 GHz radio equipment	25

3.2.2.1	Measurement setup	25
3.2.2.2	Network settings	26
3.3	LIDAR scanning	28
3.4	3D scanning of train carriage	28
3.5	Ray tracing simulations	29
3.5.1	Preprocessing of 3D file	29
3.5.2	Ray tracing simulation parameters	31
3.5.3	Ray tracing simulation setup	31
4	Results	33
4.1	Analytical method results	33
4.1.1	Shannon capacity simulation results	33
4.1.2	Interference impact results	33
4.2	Train measurement results	36
4.2.1	Heatmap representation	36
4.2.2	Radio channel characterization results	38
4.3	Ray tracing results	40
4.4	Simulations and measurements comparison	41
5	Discussion	43
5.1	Analytical method	43
5.2	Train measurements	44
5.3	Ray tracing simulations	45
5.4	Feasibility of 60 GHz access points for passenger Wi-Fi	45
5.5	Optimal antenna placement	46
5.6	Beamforming implications	46
5.7	Spatial multiplexing implications	47
5.8	3GPP 5G	47
5.9	Future market adaptation prediction	48
6	Conclusion	49
6.1	Analytic simulation results	49
6.2	Train measurements	49
6.3	Ray tracing simulations	50
6.4	Overall conclusion	50
6.5	Future work	50
	Bibliography	51
A	Appendix A	1
A.1	Measurement data	1
A.2	Extended information about measurements	3
B	Appendix B	5
B.1	Antenna size for millimeter waves	5
C	Appendix C	7
C.1	Ray tracing computational times	7

D Appendix D	9
D.1 More about channel modelling	9

List of Figures

1.1	Overview of system providing passenger Wi-Fi to a train. [courtesy of Icomera]	2
2.1	Overview of WLAN channels defined in the 802.11ad standard [9].	10
2.2	Transmit mask for 802.11ad [9]. The unit dBr denotes dB relative to the maximum spectral density of the signal.	11
2.3	Channel capacity versus the SNR. For low values of SNR, the capacity is approximately linear. For high values of SNR, it is logarithmic with respect to SNR.	15
2.4	Channel capacity versus the bandwidth for a constant power level [29, Chapter 5]. For low values of bandwidth, the capacity is linearly increasing with bandwidth, for high values of bandwidth, the gains are diminishing. This is due to the fact that with higher bandwidth, the effective SNR decreases for a fixed signal power.	16
3.1	Overview of simulation setup inside train carriage. One access point is placed in each end of the carriage. The moving client is inside the train carriage.	22
3.2	Train carriage used for measurements, located at Johanneberg, Chalmers University of Technology.	23
3.3	Inside train carriage, tables being placed on one side of the carriage, which is the setup used for the measurements.	24
3.4	Cart used for measurements, UWB positioning tag (left), laptop used for measurements (center) and access point (behind laptop screen).	26
3.5	Block diagram of measurement setup. The wireless link is between one 60 GHz radio to the other. The laptop is only used for controlling <i>Iperf</i> and data collection. The throughput is measured from one access point to the other.	27
3.6	Overview of measurement setup inside the train carriage. One access point is placed on a table, while the other one is placed on a cart.	27
3.7	Side view of FARO Focus 3D scanner standing inside train carriage. The scanners touch display is facing the camera.	28
3.8	3D point cloud file from 3D scanner measurements of the train carriage.	29
3.9	3D mesh files based on 3D scanner measurements for the train carriage used for measurements.	30
3.10	Final simplified mesh file used for ray tracing simulations. Note the significant simplification compared to figure 3.9a.	32

4.1	Channel capacity in logarithmic scale, comparison between a typical 5 GHz WLAN system and 60 GHz WLAN system. The maximum allowed indoor output power for the ETSI region is used. G_r denotes the client antenna gain.	34
4.2	Signal strength versus distance from two wall mounted access points inside a train carriage. One access point is mounted on each end of the train carriage.	34
4.3	SINR versus distance for four cases. Interference-free case, a case with adjacent channels (e.g. channels 1 and 2), maximally spaced channels (e.g. channel 1 and 4), and co-channel usage.	35
4.4	Capacity versus distance for four cases. Interference-free case, a case with adjacent channels (e.g. channels 1 and 2), maximally spaced channels (e.g. channel 1 and 4), and co-channel usage.	35
4.5	Heatmap of measured signal strength values.	37
4.6	Heatmap of measured throughput values.	37
4.7	Signal strength versus distance from access point (blue). A regression line (orange) from the least-squares regression is shown for the modelled path loss.	38
4.8	CDF of measured fading. Blue line is a fitted normal distribution, the orange is the empirical CDF.	39
4.9	Histogram over the shadow fading, X_σ . Normalized so that the sum of all bars are equal to one.	39
4.10	Heatmap of signal strength [dBm/m^2] from ray tracing simulations, based on the LIDAR scanned train carriage model. The results show the same characteristics as the measurements.	40
4.11	Heatmap of signal strength [dBm/m^3] from ray tracing simulations, based on the simplified train carriage model. The results show the same characteristics as the measurements.	41
A.1	Measured signal strength versus distance for the six runs used for the data analysis. From train carriage measurements.	1
A.2	Measured TCP throughput versus distance for the six runs used for the data analysis.. From train carriage measurements.	2
A.3	Position measurements from UWB positioning system for train carriage measurements.	2
D.1	Overview of channel modeling approaches [43].	9

List of Tables

2.1	Attenuation loss in materials for 60 GHz and 2.5 GHz [30]. The loss is normalized to obtain attenuation per centimeter.	8
2.2	Comparison between 802.11ad and 802.11ay standards	10
3.1	Key performance indicators for feasibility study and target values. . .	20
3.2	Parameter values used for simulation performed for comparison between an 802.11ad and an 802.11ac system.	21
3.3	Specifications and settings for 60 GHz transceiver equipment used for measurements	25
3.4	Parameter values for ray tracing simulations.	32
4.1	Capacity performance degradation compared to interference free case for different channel usage. Based on results from interference study. .	36
4.2	Measured path loss exponent, n , and standard deviation of the shadowing, σ_s for 60 GHz channel.	38
A.1	Summary of measurement series performed.	3
C.1	Summary of computational times.	7
C.2	Specifications of PC used for simulations	7

List of Abbreviations

AP	Access Point
dBm	decibel referenced to 1 milliwatt (mW)
EIRP	Equivalent Isotropically Radiated Power
ETSI	European Telecommunications Standards Institute
FCC	Federal Communications Commission
FST	Fast Session Transfer
IEEE	Institute of Electrical and Electronics Engineers
LIDAR	Light Detection and Ranging
LOS	Line of Sight
MTU	Maximum Transmission Unit
OFDM	Orthogonal Frequency Division Multiplexing
PL	Path Loss
SNR	Signal to Noise Ratio
TCP	Transmission Control Protocol
UDP	User Datagram Protocol
WLAN	Wireless Local Area Network

1

Introduction

In today's world, Internet connectivity is expected everywhere, including on public transportation such as trains. From the train operator's perspective there is also an incentive to provide connectivity as a service to passengers. In a study by [1], 72% of business travelers asked, replied that they were more likely to use trains compared to airplanes or cars if Wi-Fi access was available on board trains [1]. It has also been predicted in a case study that the number of trips taken was 2.7% higher than it would have been without free Wi-Fi [2]. New riders were found to make an estimated 8.6% more trips than if Wi-Fi was not available [2]. Wi-Fi will still play an important role as a complement to cellular connectivity for users. A survey from November 2017 showed that even users with unlimited cellular data plans got the majority of their traffic via Wi-Fi rather than cellular [3]. For users with smaller data plans (< 5 GB/month), Wi-Fi data corresponded to about 90% or more of the total usage [3]. Cisco has predicted that in 2021, 63% of traffic from dual-mode devices such as smartphones and tablets, excluding laptops, will be over Wi-Fi or small-cell networks [4].

There are different methods of providing train passengers with Wi-Fi connectivity. Usually a train router is connected to the Internet via the cellular network, satellite link or dedicated trackside base stations. The Internet connectivity is then distributed to the passengers via on board Wi-Fi access points. In the methods described, the access points are connected to the on board router which connects to the backhaul via roof mounted antennas. See an example of a system providing passenger Wi-Fi to trains in figure 1.1. The reason for using roof mounted antennas can be explained by that train carriages can act as Faraday cages, not allowing RF signals to propagate through into the carriage due to the metallic walls. Modern trains do also in many cases have energy-saving glass windows, which can significantly degrade the signals through the windows [5]. This means that a passenger potentially can get better performance by connecting with a system using roof mounted antennas and a type of relay instead of communicating directly through the vehicle walls or windows to exterior networks such as cellular.

With the increase of high bandwidth services such as 4K video streaming, virtual and augmented reality applications, there is a need to increase the on board access network capacity to be able to deliver a good quality of service even in the most crowded cases. The connectivity to the train which is usually provided via the cellular network will improve with further installments of LTE-Advanced and the introduction of 5G, and other solutions such as dedicated high capacity train-

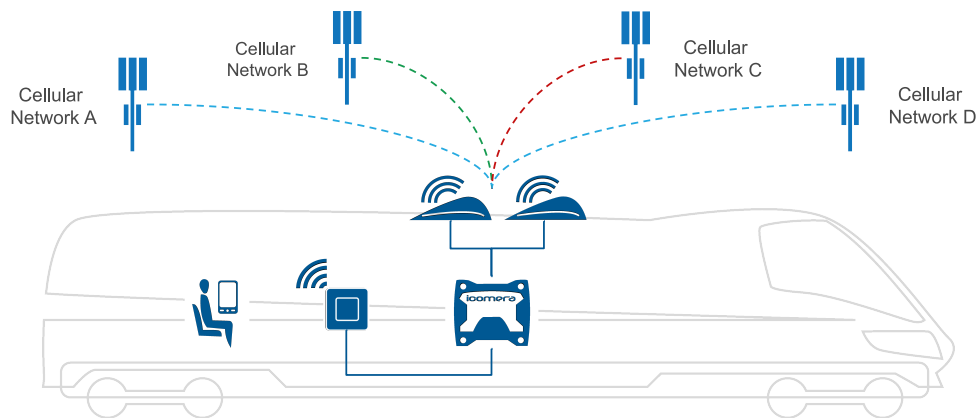


Figure 1.1: Overview of system providing passenger Wi-Fi to a train. [courtesy of Icomera]

to-ground trackside networks. Some train connectivity solutions support so called link aggregation, in which multiple links can be combined and used simultaneously [6]. Link aggregation can provide improved capacity and coverage by using multiple cellular operators in parallel.

However, the possibility to deliver high capacity to users in a crowded train carriage is a challenge due to the limited bandwidth available in the current 2.4 GHz and 5 GHz Wi-Fi bands. One solution to this problem could be to use millimeter wave communications using standards such as the IEEE 802.11ad and 802.11ay utilizing frequencies around 60 GHz, where plentiful of bandwidth is available.

In the 60 GHz band there is several gigahertz of unlicensed spectrum available for Wi-Fi (WiGig) communications [7], [8], enabling multi-gigabit capacity [8] and less interference between carriages. A 60 GHz system would also offload the 2.4 GHz and 5 GHz bands, which would also improve the experience for the users which do not have 60 GHz support. IEEE 802.11ad is a 60 GHz standard, with the capability of providing multi-gigabit capacity [9]. Recent development has led to a rise of low-cost 802.11ad devices [10]. Currently it is mainly employed in point-to-point solutions [11], [12], but there are some access points, smartphones and laptops which support the standard [13]–[15].

1.1 Motivation for millimeter waves on trains

There are several aspects in which millimeter wave communication systems have significant advantages compared to the sub 6 GHz solutions traditionally used for train carriages. The main advantage is the high achievable capacity, which is possible due to the large amount available spectrum. In the United States 7 GHz of unlicensed spectrum is available between 57 and 64 GHz [7], and in the ETSI region 9 GHz of bandwidth is available [8]. The 802.11ad standards has a channel bandwidth of

2.16 GHz [9], which can be compared to a maximum channel bandwidth of 160 MHz in current sub 6 GHz Wi-Fi standards [16]. Hence, even by using simple modulation schemes it is possible to reach high capacity due to the sheer amount of spectrum.

One issue with current solutions is interference between carriages. 60 GHz signals experience high attenuation in many wall materials and energy saving windows. Hence, the overhearing from one carriage to another can be significantly smaller compared to sub 6 GHz systems. Due to the higher material attenuation of millimeter waves, it might also be possible to deploy more dense cells. A scenario with two access points or more per carriage operating at the same frequency band is possible. To conclude, the usage of 60 GHz access points for passenger Wi-Fi has the potential to improve the whole system throughput by an order of magnitude, and decrease the issues with interference between carriages.

1.2 Challenges of millimeter wave communications

There are some aspects of millimeter wave technology which can be seen as drawbacks compared to sub 6 GHz systems. The high attenuation will reduce the effective range of a cell for a given output power and antenna gain. In the 60 GHz band, a human body attenuates a signal by approximately 20 to 30 dB [17]. The human body attenuation will significantly reduce the possibility of having a stable high capacity connection in some cases. However, in modern millimeter wave systems, techniques such as beamforming can partly mitigate this effect by directing the beam and forming alternative signal paths. If there are several access points in a room, body blockage to one access point might not be a problem since the user still can connect to another access point.

Another aspect is the oxygen absorption of frequencies around 60 GHz [18], which is between 15 to 30 dB/km [19], however for a distance less than 100 m between the access point and a client, the loss due to oxygen absorption is less than 1.5 to 3 dB, which is negligible in many cases. Due to the fact that line of sight between the access point and the client device is often required for high capacity communication, the placement of access point antennas are more crucial for 60 GHz than for sub 6 GHz standards. Another difference is that for sub 6 GHz systems, it is often possible to use external antennas, which are connected to access points via coaxial cables. However, for 60 GHz systems, this is in general not feasible due to the high cable losses associated with 60 GHz signals through coaxial cables. In 60 GHz solutions, the antenna is in many cases directly integrated with the RF frontend on the same chip.

1.3 Scope

This study is focused on investigating the technical feasibility of providing passenger Wi-Fi with 60 GHz access points. This is in part done by performing radio measurements and ray tracing simulations to determine the radio characteristics.

Interference between adjacent access points is also investigated. The physical and technical limitations are the primary focus, rather than economical. Communication systems using the 60 GHz band utilizing IEEE 802.11 WLAN standards are primarily covered. The usage and implications of other millimeter wave frequencies and standards are discussed. The performed measurements are limited to one type of train carriage. All the measurements are performed using equipment based on 802.11ad. IEEE 802.11ay is covered theoretically. For the simulations, the channel capacity is considered, with a certain implementation loss to take the hardware and software constraints into account. A train carriage 3D model is created by a LIDAR-scanning. The 3D model is used for ray tracing simulations done in *COM-SOL Multiphysics*.

1.4 Thesis Aim and Contribution

This thesis aims to investigate the feasibility of using 60 GHz access points on board trains for passenger access. According to [10], much has been investigated in the 60 GHz area, but there is still a lack of insight on how to build 802.11ad networks [10]. This thesis aims to contribute with knowledge and understanding on how to optimally build high performance 60 GHz networks for train carriages. The 60 GHz radio channel is investigated by performing propagation measurements inside a train carriage. The effects of interference on system performance is investigated through simulations. A radio channel model for 60 GHz for train carriages is developed by determining the path loss exponent and the standard deviation of the shadow fading, which could be used for future radio planning. To the best of the authors knowledge, no 60 GHz channel characterization based on measurements has been performed inside train carriages. To summarize in short, this thesis aims to achieve the following:

- Evaluate the feasibility of millimeter wave access networks on board trains for passenger access.
- Characterize the 60 GHz radio channel inside train carriages using measurements.
- Perform a system performance study for 802.11ad access points for a train carriage.
- Perform ray tracing simulations and compare the results with measurements.

1.5 Previous work

There are different types of related work that has been performed. Both theoretical analysis, in analytic studies and simulations, as well as measurements. Regarding the related measurements, they can be divided into two main categories, pure 60 GHz propagation measurements, and 802.11ad network layer measurements. The propagation measurements helps understanding the feasibility in different environments, and how different types of materials attenuate and reflect 60 GHz signals.

In [10] an empirical investigation of 802.11ad networks was performed. The study

showed gigabit-level throughputs for an indoor testbed. Adjacent Channel Interference (ACI) and Co-Channel Interference (CCI) measurements were also conducted, which showed a significant performance decrease due to both ACI and CCI.

In [20][21] measurements were performed in airplane cabins. In [22] a channel sounding study was performed inside a bus coach to determine the frequency-domain channel. In [23] the data throughput is measured inside a modern car, for different fixed positions. All the measurement campaigns mentioned used different methods when performing the measurements. Hence even if the environments are similar to what is used in this work, the measurement setup is different. To conclude, there has been some millimeter wave measurements performed in environments similar to train carriages. However, they are all performed with different measurement methodologies. In [24] the effects of human activity on 60 GHz indoor radio channel was investigated, and a significant outage probability due to humans being active inside in an indoor environment was determined.

In [25] several analyses have been made including propagation simulation for 60 GHz inside train carriages by using ray tracing methods. Performing measurements is mentioned as future work. In [26], simulations for both coverage and spectral efficiency of ultra-dense millimeter wave ceiling mounted access points, taking both human blockage and interference into account was performed. In [26] a system model was created to determine an optimal distance between access points. In [27] simulations for wearables (smart watches and such) inside a train carriage have been performed, with human blockage taken into account. To conclude, there has been numerous simulation works done for millimeter waves inside train carriages, but no rigorous measurement campaigns for 60 GHz has been performed to the best of the author's knowledge.

2

Theoretical background

This chapter gives an overview of current millimeter wave communication systems. An overview of 60 GHz wave propagation characteristics is provided, as well as sections about the IEEE 802.11ad and 802.11ay standards. The current spectrum regulations for WLAN communications in the 60 GHz band is mentioned. Finally, there is a section dealing with capacity calculations.

2.1 Millimeter wave communications

Millimeter wave (mmWave) communication systems usually refers to technology utilizing frequencies between 30 and 300 GHz [18]. In recent years millimeter wave systems have started to gain traction in the communications area due to advances in process technologies and integration solutions allowing for more cost effective products [18]. Today millimeter wave technology is used extensively in point-to-point communications in backhaul applications [18], as an alternative to running optical fiber. Millimeter wave outdoor fixed point-to-point radio links can allow for a low installation cost compared to optical fiber installations, whilst still allowing for a high capacity. Millimeter waves will be a part of the next generation cellular standard, 5G. Frequency bands around 28 GHz, 37 GHz and 39 GHz are considered to be used in 5G in the United States [28]. The 60 GHz band is as of today used in communication for both backhaul applications, as well as WLAN applications. The IEEE 802.11ad WLAN communication standard uses the 60 GHz band [9]. The focus of future applications is often in the access network, providing connectivity to the end user devices such as smartphones and laptops. This is made possible due to the decrease in cost [10], which allows the communication modules to be implemented in devices.

Most modern access network communication systems such as LTE or Wi-Fi utilize sub 6 GHz frequencies. There are several important differences between sub 6 GHz systems and millimeter wave systems. One difference is the physical size of the actual components. The size of an antenna is related to the wavelength. Using formulas described in appendix B and assuming constant radiation and aperture efficiencies, it can be shown that the area of an antenna utilizing 5 GHz band, such as some Wi-Fi standards, have a physical antenna area which is more than one hundred times larger than an antenna with an equivalent gain for the 60 GHz band. The fact that antennas in general are very small for 60 GHz systems allows for much more compact receiver and transmitter systems. At sub 6 GHz bands, a few hundred

megahertz of unlicensed spectrum is available in most regions of the world, however at around 60 GHz several gigahertz of unlicensed spectrum is available. This gives the possibility of a very high throughput since the capacity is proportional to the available spectrum for high values of signal-to-noise ratio [29, Chapter 5].

2.2 60 GHz wave propagation

In general it can be stated that 60 GHz waves can be viewed as optical or quasi-optical, in the sense that many common solid materials significantly attenuate signals [18]. In table 2.1 the measured attenuation for a few materials is shown from a campaign performed at Virginia Tech [30]. It can be noted that according to these measurements, all materials tested, except clear glass, 60 GHz signals are more attenuated than 2.5 GHz signals. This study shows that some materials have almost the same attenuation for sub 6 GHz signals as for 60 GHz signals [30]. Many authors such as [10] state that there is high attenuation of 60 GHz signals. Although this may be true for many common materials, for network planning, it is important to remember that some materials can have almost the same attenuation for sub 6 GHz signals as for millimeter waves [30]. This is further supported by another study made on car windows for frequencies between 50 GHz to 110 GHz, only measured a loss of between 2 dB for 60 GHz signal with a 0 degree incident angle [31]. There has been a lot of 60 GHz wave propagation and attenuation measurements performed for different materials and environments. Various methodologies have been employed, but in general a setup with well defined antennas (such as horn antennas) are used in conjunction with vector network analyzers (VNA's).

Table 2.1: Attenuation loss in materials for 60 GHz and 2.5 GHz [30]. The loss is normalized to obtain attenuation per centimeter.

Attenuation loss	60 GHz	2.5 GHz
Drywall	2.4 dB/cm	2.1 dB/cm
Standard office whiteboard	5.0 dB/cm	0.3 dB/cm
Clear glass (3.175 mm thickness)	11.3 dB/cm	20.0 dB/cm
Mesh glass (3.175 mm thickness)	31.9 dB/cm	24.1 dB/cm

Another important characteristic to consider is the reflection properties of different materials. This will determine how feasible non-line of sight (NLOS) communication is. If all the energy would be absorbed by the first reflection, NLOS communications would not be possible. Based on studies such as [32] it can be stated that for example metal acts as a very good reflector, whilst materials such as carpets and drywall has worse reflection properties [32]. In [24] the authors investigated the effects of human activity for an indoor 60 GHz connection among zero and up fifteen persons. For this scenario, the connection was "unavailable" for 1 % to 2 % of the time when there was one to five persons in the room [24]. Another study investigated four body types and found an average attenuation of 22 dB [33]. From this it is possible to conclude that human body blockage will have a significant impact on performance, if the line of sight is blocked.

It may not be possible to guarantee one hundred percent coverage of a 60 GHz system. However this is resolved by the fast session transfer feature which can be implemented in 802.11ad devices, which allows a device to rapidly switch to the 5 or 2.4 GHz band. One study [18] predicts a range of about 10 m for indoor usage of 60 GHz WLAN and 500 m to 1000 m for outdoor usage in point-to-point solutions, based on old spectrum regulations.

At the current market, there are several point-to-point solutions claiming distances of up to 1.6 km by using high gain reflector antennas [11]. However it is important to note that these solutions are very sensitive to antenna miss alignment due to the very narrow beamwidth being used. There are also some more flexible solutions using beamforming [12], providing ranges of up to about 200 m to 300 m, whilst allowing for a moving client due to beamforming being used instead of a passive antenna. The actual achievable performance will also be region dependent, due to regulatory differences.

2.3 IEEE millimeter wave standards

An IEEE task group has developed one standard for millimeter wave WLAN, and there is currently another task group working on an amendment which contains several improvements. The two communication standards for WLAN are discussed in this section. These standards are sometimes referred to as WiGig, which is a term that originated from a trade association called Wireless Gigabit Alliance which promoted 802.11ad. The association was in 2013 merged with the Wi-Fi Alliance. The Wi-Fi alliance now offers WiGig certifications for devices similar to what is provided to other Wi-Fi standards [34].

2.3.1 802.11ad

IEEE 802.11ad is a WLAN standard using the 60 GHz band aimed at providing multi-gigabit connectivity [35]. 802.11ad is currently commonly used in point-to-point solutions [11], [12], and in a few cases access points, smartphones and laptops [13]–[15]. The final standard was released in 2012, with another amendment being added in 2014 [9]. The standard is an amendment to the 802.11 standard, and hence has a lot in common with other 802.11 standards. The standard has several transmission modes. There are two single carrier modes and one OFDM mode. There is one low power single carrier mode (Low-power SC PHY), and one regular single carrier mode (SC PHY). The SC PHY is what is most commonly used in current products available on the market. The OFDM mode (OFDM PHY) is optional according to the standard. There is also a control PHY which is mainly used during beamforming training. 802.11ad has a maximum PHY capacity of 7 Gbit/s [9], although most available products only support a PHY capacity of 4.6 Gbit/s.

2.3.2 802.11ay

IEEE 802.11ay is an amendment to 802.11ad which aims to increase the capacity from 7 Gbit/s to 30 Gbit/s [36]. 802.11ay implements several improvements which allows for a higher theoretical capacity. Two of the major advances compared to 802.11ad is the introduction of MIMO and channel bonding [37]. The design target of the 802.11ay task group is to have at least one transmission mode which supports at least 20 Gbit/s [37]. The new maximum capacity is under the constraint that the power efficiency per station should be maintained or improved compared to 802.11ad [37].

Table 2.2: Comparison between 802.11ad and 802.11ay standards

	802.11ad	802.11ay
Final standard release date	2012 [9]	2019 (estimated)
Standard draft 1.0 release date	2009	2017 [37]
Highest modulation scheme	64-QAM [9]	TBD
Maximum capacity	7 Gbit/s [9]	30 Gbit/s [36]

2.3.3 WLAN channels

There are four 2.16 GHz wide channels defined in the 802.11ad standard [9], shown in 2.1. The availability depends on the geographical region of operation. A compliant client should support at least channel 2 [9]. The channel bandwidth in 802.11ad is much higher than the channel bandwidths used in sub 6 GHz Wi-Fi standards such as 802.11ac. In 802.11ac a mandatory bandwidth of 80 MHz and an optional of 160 MHz is specified [16].

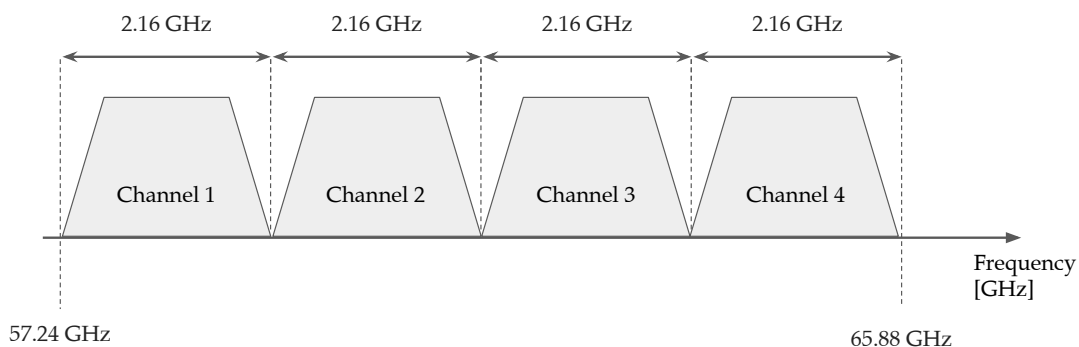


Figure 2.1: Overview of WLAN channels defined in the 802.11ad standard [9].

The Wi-Fi Alliance has specified a total of six channels for WiGig [38], hence, two more than specified in the 802.11ad standard. The channels range from 57 GHz to 71 GHz [38].

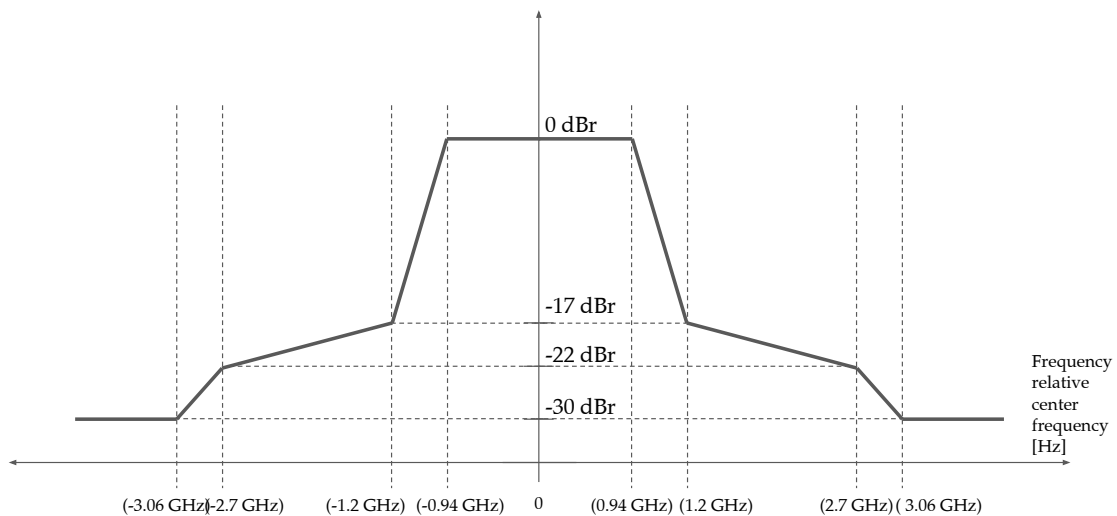


Figure 2.2: Transmit mask for 802.11ad [9]. The unit dBr denotes dB relative to the maximum spectral density of the signal.

2.3.4 Transmit mask

The transmit mask specifies how much out of band transmitted power is allowed in the standard. This will determine how much interference a compliant transmitter can cause to adjacent bands. To be able to calculate the interference between access points, the transmit mask can be used [39]. The transmit mask for 802.11ad is specified in [9]. The spectral mask is defined for a resolution bandwidth of 1 MHz, and that the measured data packets should be longer than $10 \mu\text{s}$, without training fields [9]. It can be seen in figure 2.2 that adjacent bands can disturb each other from -22 to -17 dB relative to the maximum power. However, by using far spaced bands, such as channel 1 and 4, which are spaced by 6.48 GHz, the out of bands emissions are at least -30 dB below the maximum transmitted power. The out of band emissions could potentially degrade the performance due to the increased interference. How large the effects of interference will be depends on the receiver filters, path loss between the disturber and receiver, and other factors.

2.3.5 Channel access method

The channel access method concerns how users share and access the channel in a communication system. To be able to predict the performance for a system with multiple users, it is necessary to consider the channel access method used. IEEE 802.11 employ Carrier Sense Multiple Access with Collision Avoidance (CSMA/CA) [40]. In CSMA/CA a device listens before trying to transmit (carrier sensing), and waits if the channel is found to be busy. 802.11 has an optional feature with Request-to-send (RTS) and Clear-to-send (CTS) [40]. A client wishing to transmit data will in this case send an RTS, and if the access point is available, it will send a CTS to the client, indicating that the specific client is allowed to transmit. In wireless

networking the so-called hidden node problem [40] occurs when clients both can reach a certain access point, but not each other. This situation is resolved by the usage of RTS/CTS, since the access point can hear both clients, and arrange the communication.

2.3.6 Fast Session Transfer

Fast Session Transfer (FST) is a feature in 802.11ad which allows a device to rapidly switch from one band (e.g. 60 GHz band) to another (5 GHz or 2.4 GHz bands) seamlessly [41]. Hence, a supported device can always use a sub 6 GHz band as fallback if losing 60 GHz coverage.

2.4 Spectrum regulations

The regulations related to the usage of the frequency bands have a significant impact on the performance which can be achieved. There are in general different rules for outdoor and indoor usage, and if the links are fixed (point-to-point) or not. In this section indoor usage will be considered.

2.4.1 European region (ETSI)

European Telecommunications Standards Institute (ETSI) is a standardization organization. The ETSI standards are an attempt at creating harmonised European standards. To avoid details, it can be said that most European countries follow the ETSI standards or a modified version of the standards. The rules related to indoor usage of the 60 GHz band for WLAN applications are specified in [8]. This document defines the 60 GHz band as frequencies, typically from 57 GHz to 66 GHz. The regulation specifies a maximum mean RF output power of 40 dBm Equivalent Isotropically Radiated Power (EIRP) for indoor usage. The RF output power is defined as the mean EIRP during a transmission burst [8]. For systems utilizing beamforming, this limit applies to the highest possible EIRP value for the antenna. For fixed outdoor links, higher EIRP levels are allowed, which allows for long range point-to-point links.

2.4.2 USA (FCC)

Federal Communications Commission (FCC) decides the regulations for the United States. These regulations are also adopted by several other countries. The rules related to the 60 GHz band are specified in "Part 15 Rules for Unlicensed Operation in the 57-64 GHz Band" [7], which state an average output power of 40 dBm EIRP and a peak output power of 43 dBm EIRP for indoor usage. The available unlicensed bandwidth is 7 GHz. Hence both the FCC and ETSI has specified a maximum mean EIRP of 40 dBm for indoor usage. For fixed outdoor links, much higher EIRP levels are allowed. For fixed outdoor links, the maximum allowed mean EIRP increases

with the antenna gain up to a certain limit, which extends the range of point-to-point radio links. More specifically, for fixed outdoor links, the maximum mean EIRP is 82 dBm minus 2 dB for each dB that the antenna gain is below 51 dBi [7].

2.5 Wireless channel modeling

Wireless channel models are useful for communication system design. They provide a way to estimate the achievable performance for different environments. There are many different types of channel models, all with their advantages and disadvantages. Channel modelling can be divided into two main branches, deterministic and stochastic [42]. As common in modelling, there is a trade off between accuracy and simplicity. Capturing all radio propagation effects can be very complex. There is also a trade off between generality and accuracy, a site-specific model does in most cases provide better accuracy than a more general model. There is an important difference between what is called a propagation channel model and a radio channel model. The radio channel is the propagation channel with the effects of the antennas into account [43], whilst the propagation model only concerns the channel "over the air". For example, a different radio channel can be measured if the receiving antenna used is very directional or more omni-directional. This is due to that in the first case, less reflections are captured if there are signals coming from the sides.

An example of a closed-form model is the two-ray model [43] which takes a direct ray and a ground reflection into account, rendering an analytic expression. These types of models may work for some types of environments, however when the geometry of an environment is very complex there is often no simple closed-form expressions which can be derived. Empirical models are based on measurements, the results are often very accurate for the specific measured environment. There are two main downsides with empirical models, the first one is that measurements are required, which might require a lot of time, the second downside is that the results may be site-specific [43].

In ray tracing methods, electromagnetic rays are modelled as optical rays, taking effects such as reflection and refraction into account [43]. Ray tracing uses a 3D or 2D model of the environment, taking absorption and reflection of materials into account. Ray tracing can be very computationally heavy. The factors affecting the computational time is among other things the number of rays, and how many reflections are taken into account. Hence there is a trade off between accuracy and computational time. Optimally, all the parameters of all environment materials such as walls, floors and windows should be known exactly, which may be difficult in many cases, therefore assumptions about the materials based on similar known materials have to be made. There has been a lot of previous work done comparing ray tracing simulations and measurements, with some studies finding a very high correlation between measurements and simulation such as in [44][45]. More details about channel modelling are described in Appendix D.

2.6 Capacity calculation

The channel capacity, also called Shannon capacity, provides an upper theoretical limit on how much information can reliably be transmitted over a channel [46]. In practice, it is possible to reach close to the capacity limit with the help of modern coding techniques [29, Chapter 5]. The channel capacity is given by [29, Chapter 5]

$$C = B \log_2(1 + \text{SNR}) \text{ [bits/s]} \quad (2.1)$$

Where C is the channel capacity, B is the bandwidth in Hertz and SNR is the signal-to-noise ratio. By observing equation (2.1) it is possible to see that the capacity is proportional to the bandwidth, and has a dependence on the SNR. However, for a fixed power level, the SNR also depends on the bandwidth. This is due to the fact that the noise depends on the system bandwidth. The SNR for an receiver can also be expressed as a ratio between the received power and the bandwidth, via the expression

$$\text{SNR} = \frac{P_{in}}{kT_e B}, \quad (2.2)$$

where T_e here is an equivalent temperature taking both the ambient temperature, and the receiver noise figure into account. k is Boltzmann constant and B is the bandwidth in Hertz. It can therefore be seen that the SNR is a function of the bandwidth, given a constant total power level.

Another way to represent the SNR is to use a receiver noise figure, an implementation loss and just thermal noise. The SNR can then in decibel be calculated as

$$\text{SNR} = P_{in} - \text{NF} - \text{IL} - kT_0 B \text{ [dB]}, \quad (2.3)$$

where P_{in} is the received power, NF is the receiver noise figure (which takes into account how much noise the receiver adds) and IL is the implementation loss. The input power, P_{in} , is given by

$$P_{in} = P_{out} + G_r + G_t - \text{PL(d)} \text{ [dBW]}, \quad (2.4)$$

where P_{out} is the output power from the transmitter and G_r and G_t are the receive and transmit antenna gains respectively. PL(d) is the path loss in decibel as a function of the distance. The path loss could be estimated by several different path loss models, such as Friis equation (free space loss), two ray model [46, Chapter 4], Okumura–Hata model, or modified Friis equation. The choice of model depends on the environment in which the communication system will be deployed.

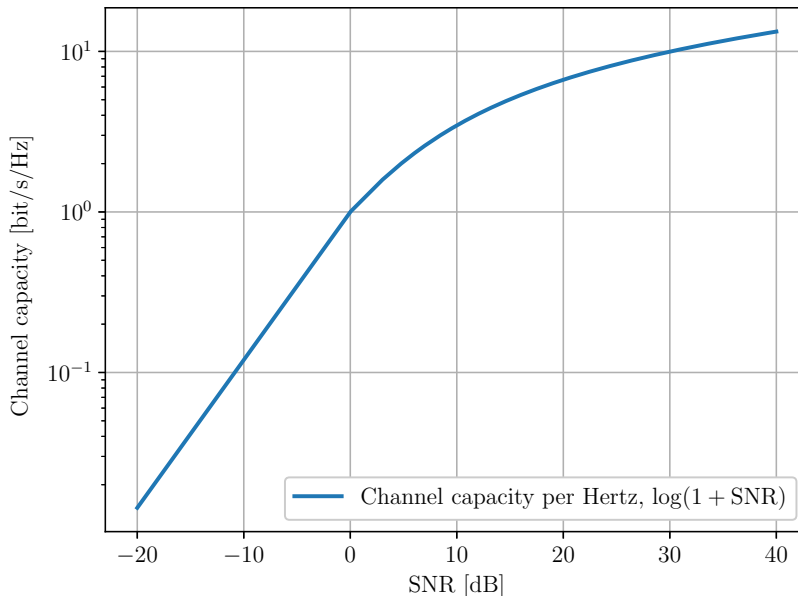


Figure 2.3: Channel capacity versus the SNR. For low values of SNR, the capacity is approximately linear. For high values of SNR, it is logarithmic with respect to SNR.

In figure (2.3) the channel capacity is shown. It can be seen that for low values of SNR, the capacity is approximately linear with respect to SNR. This is the so called linear region, or power limited, region. In the power limited region, the capacity can be increased significantly by increasing the amount of power. For higher values of SNR, the capacity is approximately logarithmic with respect to SNR. This is the so called bandwidth limited region [29, Chapter 5] (also called high SNR region). In the bandwidth limited region, adding more power (to have a higher SNR) will only marginally increase the capacity, however the capacity is directly proportional to the bandwidth. This can be shown by that for low values of SNR we have [29, Chapter 5]

$$\log_2(1 + \text{SNR}) \approx \text{SNR} \log_2(e), \quad \text{SNR} \approx 0 \quad (2.5)$$

Whilst for high values of SNR, we obtain [29, Chapter 5]

$$\log_2(1 + \text{SNR}) \approx \log_2(\text{SNR}), \quad \text{SNR} \gg 1 \quad (2.6)$$

Hence, by substituting equation (2.2) in the above formulas, and we obtain

$$C = B \log_2 \left(1 + \frac{P_{in}}{kT_e B} \right) \quad (2.7)$$

So, for the high SNR region, we obtain

$$C \approx B \log_2 \left(\frac{P_{in}}{kT_e B} \right) \quad (2.8)$$

Hence, the capacity will increase by adding more bandwidth. The reason is that the linear function grows faster than the logarithmic decreases, given that the argument

of the logarithmic function is high. This is illustrated in figure 2.4. As a matter of fact, for high values of SNR, the capacity is approximately linear with respect the bandwidth.

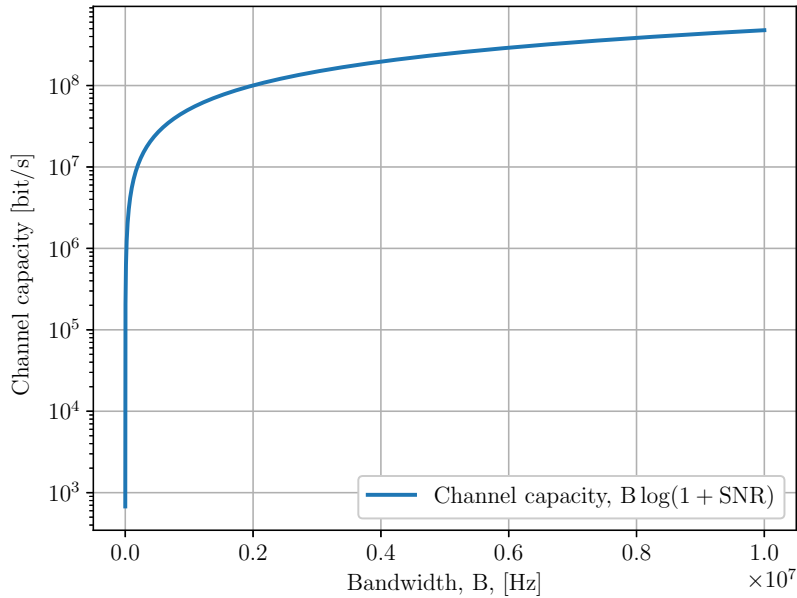


Figure 2.4: Channel capacity versus the bandwidth for a constant power level [29, Chapter 5]. For low values of bandwidth, the capacity is linearly increasing with bandwidth, for high values of bandwidth, the gains are diminishing. This is due to the fact that with higher bandwidth, the effective SNR decreases for a fixed signal power.

In general, 60 GHz communication systems have much higher channel bandwidths than sub 6 GHz systems. This explains why the capacity is much higher for a 60 GHz system compared to a sub 6 GHz system at short distances. However, by observing this equation, it can be understood that the capacity gap is closing as the distance is increasing. So in rough terms, it can be described in this way: Assuming both systems having approximately the same output power, the 60 GHz system has lower SNR due to higher bandwidth it possesses. The sub 6 GHz capacity is actually higher than the 60 GHz capacity at longer ranges, due to the lower SNR and higher attenuation in the atmosphere for the 60 GHz system.

2.7 Radio channel characterization

To be able to predict and calculate performance it is important to characterize the radio channel. In a free space case with no reflections (the so called free space loss), the following formulas describe the path loss in linear scale

$$PL(d) = \left(\frac{4\pi d}{\lambda} \right)^2, \quad (2.9)$$

which in decibels can be written as

$$\text{PL}(d) = 20 \log_{10} \left(\frac{\lambda}{4\pi d} \right) \quad [\text{dB}] \quad (2.10)$$

d is the distance in meters, and λ is the wavelength in meters. Although very useful in for example point-to-point communication systems, and satellite communication [46, Chapter 4], this model fails to capture the effects of reflections which makes it unsuitable for many applications.

A more general model which takes reflections into account is the log-distance path loss model. In [43] a collection of channel characterizations for 60 GHz is listed for environments such as office, corridor, laboratory and open field. For the large-scale channel characterization it is common to specify the path loss by the path loss exponent, n , and the standard deviation for the shadow fading, σ_s [43]. The path loss for the log-distance model is shown below

$$\text{PL}(d) \text{ [dB]} = \overline{\text{PL}}(d) \text{ [dB]} + X_\sigma \text{ [dB]} \quad (2.11)$$

$\overline{\text{PL}}(d)$ is the average path loss, X_σ is the shadow fading. To determine the path loss exponent for a case without any specific obstruction by objects [43], which represents no shadowing case, the average path loss can be modelled as

$$\overline{\text{PL}}(d) \text{ [dB]} = \text{PL}(d_0) \text{ [dB]} + 10n \log_{10} \left(\frac{d}{d_0} \right), \text{ for } d > d_0 \quad (2.12)$$

The path loss exponent can be found by performing the least squares linear regression of the measured data points [43]. A value of $d_0 = 1$ m is used commonly [43].

2. Theoretical background

3

Methods

To answer the stated problem, three investigation methods are employed:

- Analytical system level simulations
- Ray tracing simulations based on 3D LIDAR scanned model
- Measurement campaign and analysis of results (measurements inside train carriage, analysis of measured signal strength and throughput)

There are two types of simulations performed. A ray tracing part using *COM-SOL Multiphysics* [47], and capacity simulations using the programming language *Python*. The capacity simulations will consider the physical parameters of a 60 GHz 802.11ad communication system, with an access point and a client. The study will take power regulations into account for the ETSI region. The study answers questions about the theoretical maximal capacity, and a separate study is performed to determine the impact of co-channel and adjacent channel interference. The results will give insight about the theoretical maximal capacity which can be achieved. The results help to answer how many access points are required per carriage. The ray tracing simulations will generate a coverage map for the train carriage, and give a reference to compare to the measurements. The 3D model used for the ray tracing will be collected from a LIDAR scanning of a real train carriage.

The measurements will provide insights about how a practical system operates, with a real channel and real hardware and software constraints. The measured TCP throughput takes all the effects of the 802.11ad protocol into account, and the effective end-to-end throughput is determined. The radio channel is also determined via the measurements, which provides understanding on how 60 GHz signals propagate through a train carriage. Hence the measurements are important for understanding both the physical radio channel, as well as the implications of the 802.11ad standard.

Four key performance indicators are considered, shown in table 3.1.

Table 3.1: Key performance indicators for feasibility study and target values.

Parameter	Target value
Coverage	> 90 %
Number of users	> 30
System throughput	> 1 Gbit/s
Number of access points per carriage	< 4

It is important to consider that when trying to reach the target values of the performance indicators, some factors such as the train carriage model will play a role. One aspect is the length of the train carriage, which normally is in the range of between 20 to 30 meters. Another factor is the materials used inside the train carriage, some wall materials may reflect 60 GHz signals better than others. Some type of seating materials could also potentially act as absorbents, which could degrade the performance. The system throughput might seem a bit low, however this is due to the fact that system throughput decreases with an increasing number of users in 802.11 WLAN standards. Also, if sub 6 GHz standards are used, the system throughputs would be added for each technology. The coverage area is defined as the area where a client device can achieve at least 50 Mbit/s.

3.1 System level simulation

This chapter presents two system simulations, which has been realized by *Python* scripts. The first one simulation compares a 5 GHz WLAN system with a 60 GHz WLAN system for an interference free case. The setup simulates the case with a wall mounted access point, and a single mobile client device such as a smartphone. The system throughput in a practical system would decrease with an increasing number of users due to the medium access methods employed in 802.11. The second case investigates the effects of dense cells by looking at how interference affects performance in a 60 GHz system inside a train carriage for a scenario with two wall-mounted access points per carriage.

3.1.1 Capacity simulation

Before performing a system design it is suitable to calculate the predicted capacity. The final system throughput will be lower than this capacity limit due to protocol overhead and other factors.

In a link budget, factors such as output power regulations, antenna gain, path loss model and noise are taken into account. In order to have a certain outage probability, a fading margin is also taken into consideration in many cases. For instance, if the fast fading is assumed to be Rayleigh or Rician-distributed with a certain variance, then the fading margin can be determined by choosing an outage probability.

When evaluating the 60 GHz IEEE 802.11ad system theoretically, a 5 GHz Wi-Fi

system, using the IEEE 802.11ac standard, will be used as a benchmark. This analysis will depend on the antenna gain of both the client device and the access point. Since handheld devices such as smartphones have limited physical space for antennas, small, low-gain antennas are employed. This is also related to the fact that for devices such as smartphones, an omnidirectional antenna radiation pattern is in general desired, so that the device can communicate in all directions. However, the access point generally has more space available, and a larger antenna (e.g. antenna array) with a higher maximum gain could be used.

Table 3.2: Parameter values used for simulation performed for comparison between an 802.11ad and an 802.11ac system.

System	802.11ad (60 GHz)	802.11ac (5 GHz)
Channel bandwidth	2.16 GHz	80 MHz
Center frequency	60 GHz	5.725 GHz
EIRP	40 dBm	30 dBm
Receiver antenna gain	3 dBi	3 dBi
Receiver noise figure	6 dB	6 dB
Implementation loss	6 dB	6 dB
Ambient temperature, T_0	290 K	290 K
Number of spatial streams	1	1

The noise figure and implementation loss values for the 60 GHz system are gathered from [17], where a 60 GHz system calculation is performed. The same noise figure and implementation loss is assumed for the 5 GHz system. The channel capacity is calculated for the comparison between a 60 GHz and a 5 GHz system based on the values in table 3.2. The simulations are based on the relationship described by (2.1), (2.3), (2.4) and (2.10) in Section 2.6. The general procedure of the link calculation is covered in [48, Chapter 14], and some of the parameter values are gathered from [18] and [17].

3.1.2 System model for interference investigation

When considering cases with two or more access points (APs) per carriage, it is important to take interference into account. In this chapter, a system model is designed to evaluate the impact of interference.

Two wall mounted access points are considered, one on each side of a 20 meter long train carriage. The received interference signal from an interfering AP is calculated by the transmitted power minus the path loss and the 802.11ad transmit mask. The device-to-device interference is not taken into account for this calculation. Only AP-to-device interference is considered. This is based on the assumption that most Wi-Fi users use more downlink than uplink, which requires the AP to transmit more than it receives, and that the devices listen more than they transmit. Based on this, it is assumed that the majority of the interference comes from neighbouring access points, rather than surrounding clients.

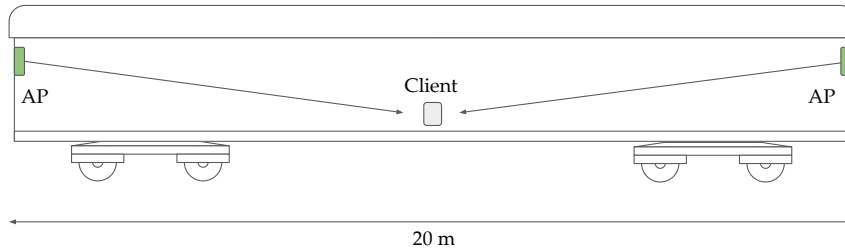


Figure 3.1: Overview of simulation setup inside train carriage. One access point is placed in each end of the carriage. The moving client is inside the train carriage.

A simple model is used in which it is assumed that the interference from one access point to the other can be seen as uncorrelated noise. The interference generated from adjacent carriages is assumed to be negligible. The idea with the model is to provide insight on how the distance, power level, and antenna type can affect the system throughput due to interference. Interference can be divided into Adjacent Channel Interference (ACI) and Co-Channel Interference (CCI) [10]. In this study, four cases are considered:

- No interference
- Adjacent channel interference (maximally spaced adjacent channel, e.g. channel 1 to 4)
- Adjacent channel interference (minimally spaced adjacent channel, e.g. channel 1 to 2)
- Co-channel interference (e.g. channel 1 to 1)

The interference model is similar to what is used in [39]. Received interference power is assumed to be the product of the output power, the gain and a factor which takes the channel overlap into consideration. The received interference power, I , can as in [39] be written as

$$I = P_{out}G\xi \quad (3.1)$$

P_{out} is the transmitted output power from the interferer, and G is the gain between the output and the input of the receiver. The gain here, G , takes path loss, antenna gains and antenna alignment mismatch into account and ξ is the channel overlap factor which takes into account how much two channels overlap. The equation can more explicitly, in decibels, be rewritten as

$$I = P_{out} - PL + G_r + G_t + \xi \quad [dB], \quad (3.2)$$

where G_r and G_t is the transmit and receive antenna gains, and PL is the path loss between the access point and the receiving device. The free space path loss model is used. The signal-to-noise plus interference (SINR) ratio is then given by

$$\text{SINR} = \frac{P_{in}}{N + I} \quad (3.3)$$



Figure 3.2: Train carriage used for measurements, located at Johanneberg, Chalmers University of Technology.

P_{in} is the input signal power, N is the noise power, and I is the interference power. The noise term N is calculated by thermal noise and an assumed noise figure of the receiver. The values of ξ are estimated from the transmit mask shown in figure 2.2. P_{in} is calculated by using the values in Table 3.2. The transmit power and antenna gain was used to determine the output power, then a channel model (free space path loss) was used and the receive antenna gain. This then determined the distance dependent value of P_{in} .

3.2 Measurements

The purpose of the measurements is to characterize the radio channel inside the train carriage. The purpose is also to test radio equipment and load the link with TCP traffic to determine the practical performance. Both these parts will help in understanding what achievable performance can be had, and help to answer whether 802.11ad-systems are feasible for passenger access.

3.2.1 Measurement campaign

Measurements were performed during February 2018 in an AB3 train carriage manufactured by ASJ for SJ, the government-owned passenger train operator in Sweden. The AB3 train carriage is situated at Johanneberg campus, Chalmers University of Technology, Sweden. The interior is modified such that the original passenger seats have been removed from the carriage, while the metal chassis and windows are in their original state. The interior and exterior of the carriage have also been repainted. The exterior of the train carriage is shown in figure 3.2, and the interior is shown in 3.3a and 3.3b.



(a) From the back of train carriage facing towards the station access point.



(b) From the front of train carriage facing away from the station access point

Figure 3.3: Inside train carriage, tables being placed on one side of the carriage, which is the setup used for the measurements.

Table 3.3: Specifications and settings for 60 GHz transceiver equipment used for measurements

Parameter	Value
Protocol	802.11ad
Channel bandwidth	2.16 GHz
Center frequency	60.48 GHz (Channel 2)
Maximum wireless capacity (PHY)	4.6 Gbit/s
Output power	14 dBm
Antenna gain	7.5 dBi approximately.
Antenna beamwidth	90° approximately.
MTU size	7912 bytes

3.2.2 60 GHz radio equipment

Two transceivers using 802.11ad operating in the 60 GHz band were used for the measurements. The specifications of the equipment, together with the used settings, are shown in table 3.3.

3.2.2.1 Measurement setup

The station access point was placed in a fixed position on a table of a height of about 1.6 m in the end of the carriage. The client access point was placed on a cart of height 1 m with wheels and was powered from a battery. During the measurements, the cart was pushed around in a controlled manner in the carriage. In total, three visits were done to the train carriage on different occasions, in which the first one acted as a test and verification run and the other two yielded high quality measurement data. For all tests, only one person, pushing the cart, was present in the carriage. The UWB positioning system uses anchor points for positioning, and a client which is the device being tracked. The manufacturers of the positioning system recommends a manual calibration of the anchor points, meaning that their actual positions are manually entered before logging starts. Manual calibration was used, and the positioning systems accuracy was verified by moving the cart around and observing that the correct positions were registered by the system. The UWB positioning anchor points were placed in the corners of the train carriage, and the client access point was placed on the cart alongside the UWB positioning tag.

The cart was placed close to the station access point, and then pulled backwards slowly to the far back of the train carriage. Then the process was then repeated for six times for different positions of the cart. Software was written to automatically record downlink and uplink TCP throughput, downlink and uplink rate, Received Signal Strength Indicator (RSSI), position and time. The software *Iperf* [49] was used for generating TCP traffic, and specific settings were configured to maximize the throughput over the wireless link. A block diagram of the measurement setup is shown in figure 3.5. An *Iperf* server was started on one of the access points, whilst the other access point was running *Iperf* in client mode. The laptop was only used for starting the *Iperf* server and client remotely via SSH, and to do the data logging.



Figure 3.4: Cart used for measurements, UWB positioning tag (left), laptop used for measurements (center) and access point (behind laptop screen).

However, the throughput was directly measured from one access point to the other, and not via the laptop to the other access point. The Linux system shown in figure 3.5 is a light-weight Linux distribution with 802.11ad drivers installed. Prior to the train measurement campaign, both the transceiver and positioning equipment was extensively verified and tested in an office environment. The initial testing showed that the measurement system was functioning as expected, and that the data logging was functioning correctly.

3.2.2.2 Network settings

Channel 2, with a center frequency of 60.48 GHz, was used for the measurements, this is the default 802.11ad channel which should be supported by all devices. In TCP traffic, the Maximum Transmission Unit (MTU) determines the maximum packet size. In general, a higher MTU size can increase the efficiency by reducing the amount of overhead. An MTU size of 7912 bytes was used to obtain high throughput values to be closer to the PHY rate. A smaller MTU would yield lower throughput values due to more overhead. This is also confirmed by preliminary tests performed with the default MTU size of 1500 bytes. TCP traffic was used for all tests; however, a higher throughput can be expected if UDP traffic was used, as observed in [10]. TCP traffic is in general used for services where the message must reach its destination such as email and web surfing, where no lost packets are acceptable. UDP is commonly used in video streaming, Voice over IP (VoIP) and some types of online gaming, where low latency is more important than low packet loss.

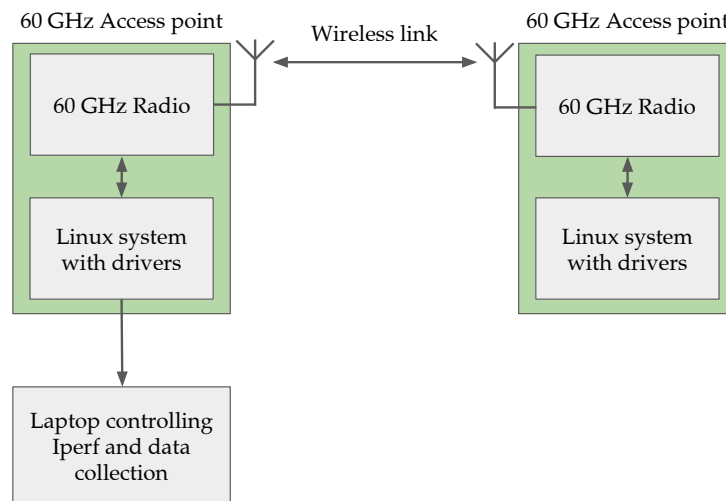


Figure 3.5: Block diagram of measurement setup. The wireless link is between one 60 GHz radio to the other. The laptop is only used for controlling *Iperf* and data collection. The throughput is measured from one access point to the other.

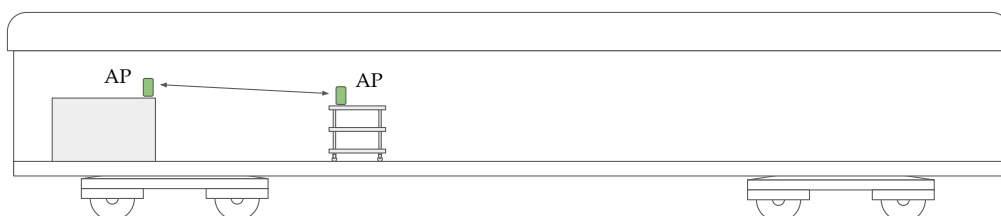


Figure 3.6: Overview of measurement setup inside the train carriage. One access point is placed on a table, while the other one is placed on a cart.

3.3 LIDAR scanning

LIDAR (Light Detection and Ranging) is a method which transmits laser pulses, and by measuring the reflected signal can measure the distance to objects. By moving the laser beam and scanning in all directions, it is possible to obtain a 3D model of the environment.

3.4 3D scanning of train carriage

A 3D model of the inside of the train was generated from a point cloud which was generated from a LIDAR scanning ("3D scanning"). A side view of the 3D scanner is shown in figure 3.7.

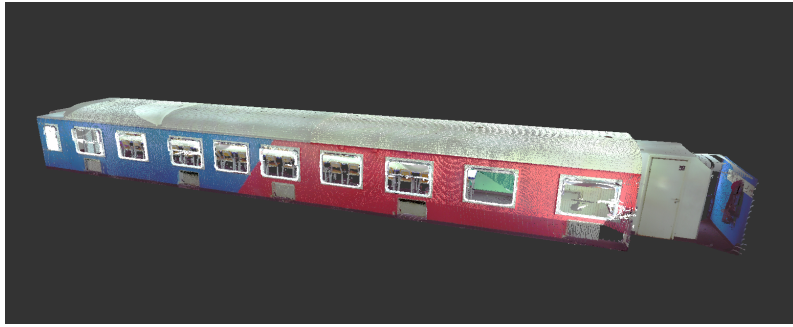


Figure 3.7: Side view of FARO Focus 3D scanner standing inside train carriage. The scanners touch display is facing the camera.

The scanning was performed by using scanner equipment ("FARO Focus 3D") from the company FARO. The scanner was placed at four different locations inside the train carriage, and the point cloud data files were then merged into one large point cloud. The result is a high-resolution colored 3D point cloud of the trains interior.

The point cloud observed from a distance is shown in figure 3.8a, and the point cloud viewed from inside the train is shown in Figure 3.8b. The colored capture is possible since a digital camera is integrated with the LIDAR scanner which maps the color data into the corresponding cloud points. The scanning successfully captured the details of the interior of the train carriage. Features such as the arcs in the ceiling was successfully captured, which can be observed by comparing figure 3.3a and 3.8b.

The point cloud files were processed with the software *CloudCompare* [50] to generate 3D mesh files by the poisson surface reconstruction function. The mesh files uses 3-dimensional sections instead of points. The purpose of this is that ray tracing software in general requires solid 3D models, and does not function with point cloud models. The surface reconstruction parameters were tweaked until a result which



(a) From the outside of train carriage. Note that the point cloud is only based on the scanning performed on the inside of the carriage.



(b) From inside of the train carriage used for measurements. Note that details such as the arcs in the ceiling have been successfully depicted.

Figure 3.8: 3D point cloud file from 3D scanner measurements of the train carriage.

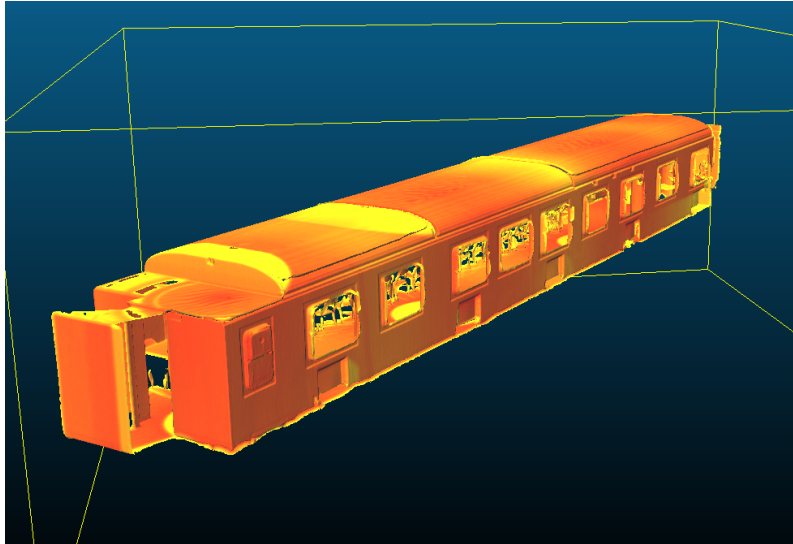
provided a good level of detail and surface smoothness was achieved. The mesh format files are shown in figures 3.9a and 3.9b.

3.5 Ray tracing simulations

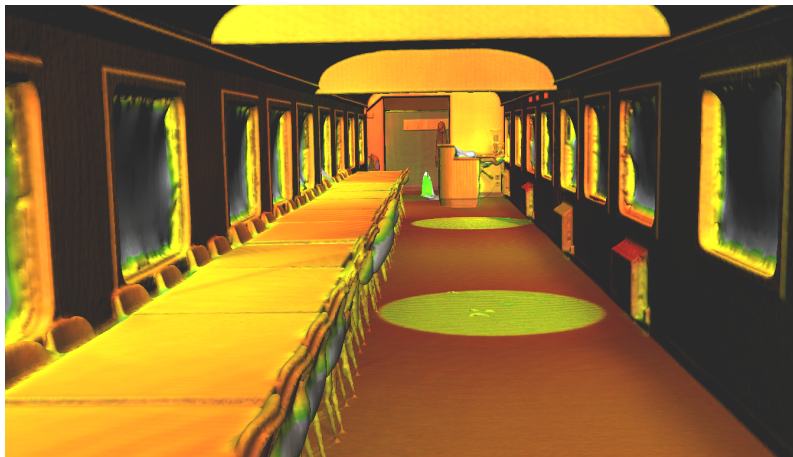
Ray tracing simulations using *COMSOL Multiphysics* were performed to evaluate the coverage inside the train carriage for 60 GHz.

3.5.1 Preprocessing of 3D file

The 3D file from a LIDAR scanning was used. The raw 3D mesh file was too large in file size to directly be used for the simulations. Instead, the number of mesh elements were reduced until the file reached a manageable size. Here, there is a trade off between model accuracy, file size and computational efficiency. A manually built simple 3D model was also set as a reference for comparison.



(a) From outside of train carriage.



(b) From inside of the train carriage used for measurements. Note that details such as the arcs in the ceiling have been successfully depicted.

Figure 3.9: 3D mesh files based on 3D scanner measurements for the train carriage used for measurements.

3.5.2 Ray tracing simulation parameters

When discussing optical reflection, it is common to divide reflections into so called specular reflections, and diffuse reflections. In specular reflection the outgoing reflected ray is reflected with the same angle as the incoming ray. This is normally found in very even surfaces such as iron, glass etc. Diffuse reflections captures the effects of rough surfaces, so that the outgoing rays have an outgoing angle which is random. The reflection of the walls were determined such that a certain amount of the incoming rays experienced specular reflections, whilst the others experienced diffuse reflections. A certain loss (absorption constant) was set for all walls, to emulate the real behaviour of lossy walls. When running the simulation, there are a lot of parameters to be set, see table 3.4. For example, the number of outgoing rays, radiation pattern, wall reflection parameters, mesh size, etc. It is in some sense difficult to replicate all these parameters perfectly to reflect what was used for the measurements.

3.5.3 Ray tracing simulation setup

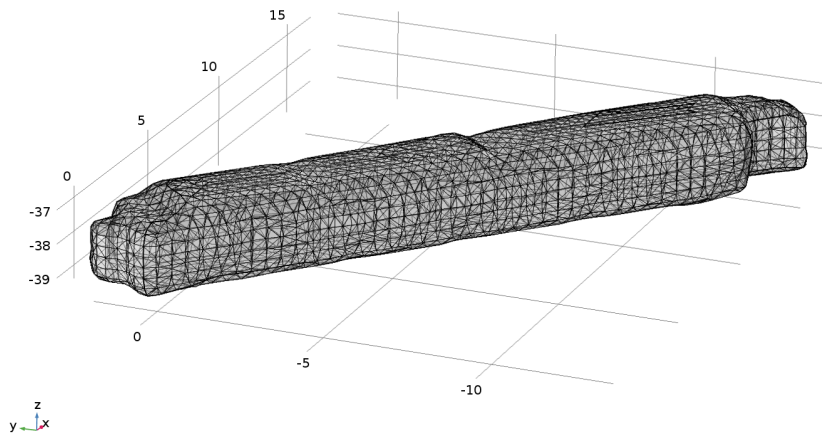
This section explains how the ray tracing simulations were performed. An absorption coefficient of 0.2 is used for all walls during the simulations. The value was chosen so that the simulation results were similar to the measurements. This means that the rays lose 20 % of their energy at each reflection. This means that there is an assumption that the walls are very reflective for 60 GHz waves, or at least that the propagation can be explained by this behaviour.

Specular reflection is mainly used in the simulations, since this was found to produce results most close the measurements. This can be explained by that the walls have a quite even surface. Each ray has a 90 % chance of specular reflection and a 10 % chance of diffuse reflection. The outgoing ray pattern is made to emulate the radiation pattern of the antenna used for the measurements.

The main ray tracing settings used are summarized in table 3.4. The signal strength is found for a plane which is at about 1 metre over the floor of the train carriage, which approximately at the same height as the access point in the measurements. The "receive antenna" used in the simulations is isotropic, in the sense that the received power is calculated from rays from all directions. However, it is assumed that most of the received energy is coming from the direction of the access point antenna. Because of this, the results can be estimated to be close to what would have been if the same radiation pattern as for the antenna used during the measurements had been used.

Table 3.4: Parameter values for ray tracing simulations.

Parameter	Value
Specular reflection percentage	90 %
Diffuse reflection percentage	10 %
Number of rays	5000
Time for power accumulation	300 ns
Ray energy loss per reflection	20 %

**Figure 3.10:** Final simplified mesh file used for ray tracing simulations. Note the significant simplification compared to figure 3.9a.

4

Results

This chapter shows the results from the simulations and measurements. First the results from the analytical method are presented. After that the train measurement results are presented, both with heatmaps and other types of data visualization. Lastly, the ray tracing results are shown in the form of heatmaps.

4.1 Analytical method results

4.1.1 Shannon capacity simulation results

This section covers the results from the analytical simulations performed. Figure 4.1 shows the maximum theoretical capacity, the so called Shannon capacity, for a 60 GHz WLAN system (e.g. 802.11ad) and a 5 GHz system (e.g. 802.11ac) for a free-space channel model. For this simulation setup, the distance where the 5 GHz system performs better is found to be at 350 m, which can be seen in figure 4.1. For distances less than 20 m, which is approximately the length of a train carriage, the 60 GHz system can achieve over 10 Gbit/s theoretically. It is not possible to achieve the channel capacity in practice; 802.11 standards have a significant overhead which will reduce the effective throughput. It can be seen from figure 4.1 that the capacity drops rapidly with increasing distance.

The differences between the 60 GHz and the 5 GHz systems are the bandwidth, center frequency and output power, with the rest of the parameters assumed to be the same. The reason why the 60 GHz system has a much higher capacity at short ranges is its bandwidth which is more than 20 times larger than the 5 GHz system.

4.1.2 Interference impact results

The received signal strength values of the two access points are shown in figure 4.2. Each AP is assumed to be mounted on each end of the train carriage. The SINR for one of the access points is shown in figure 4.3. The capacity, based on the SINR values, is shown in figure 4.4. The capacity is calculated using equation (2.1). It can be noted that co-channel usage suffers a significant reduction in capacity. However, by using different channels, even closely spaced channels, the performance is not significantly degraded. It shows that two access points, mounted inside a train carriage on each end, can affect each others performance significantly. If adjacent channels are used (e.g. channel 1 and 2), the Shannon capacity is reduced by a few

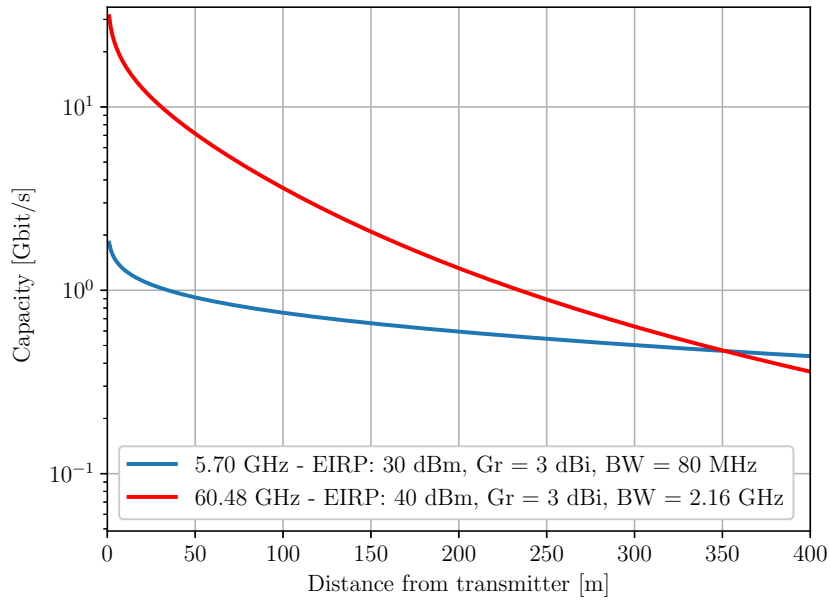


Figure 4.1: Channel capacity in logarithmic scale, comparison between a typical 5 GHz WLAN system and 60 GHz WLAN system. The maximum allowed indoor output power for the ETSI region is used. Gr denotes the client antenna gain.

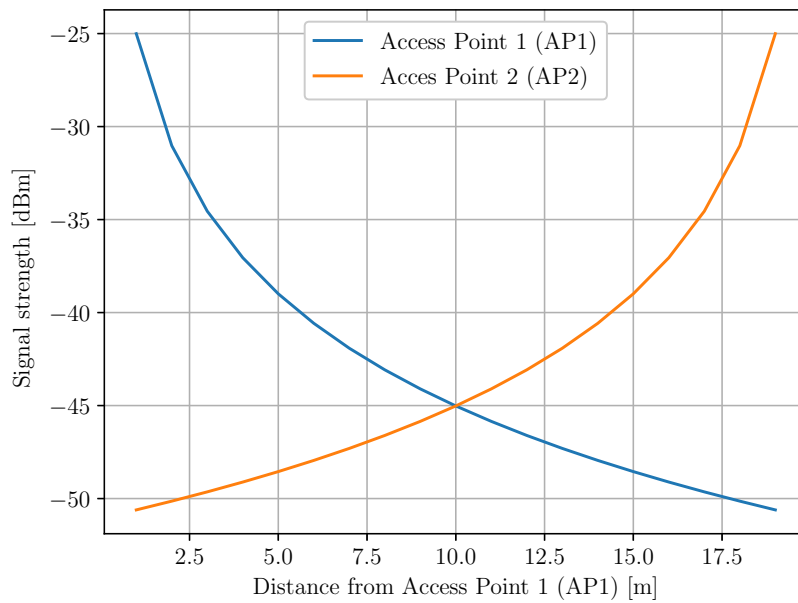


Figure 4.2: Signal strength versus distance from two wall mounted access points inside a train carriage. One access point is mounted on each end of the train carriage.

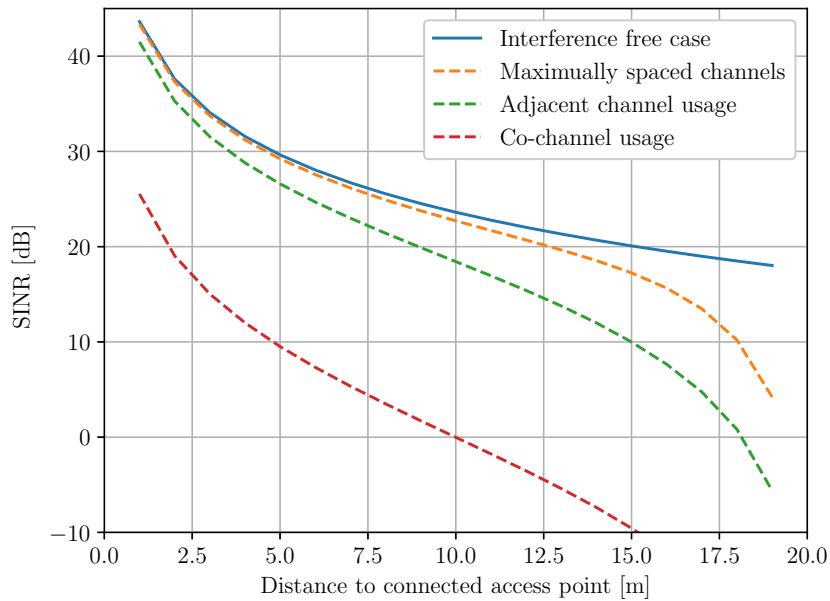


Figure 4.3: SINR versus distance for four cases. Interference-free case, a case with adjacent channels (e.g. channels 1 and 2), maximally spaced channels (e.g. channel 1 and 4), and co-channel usage.

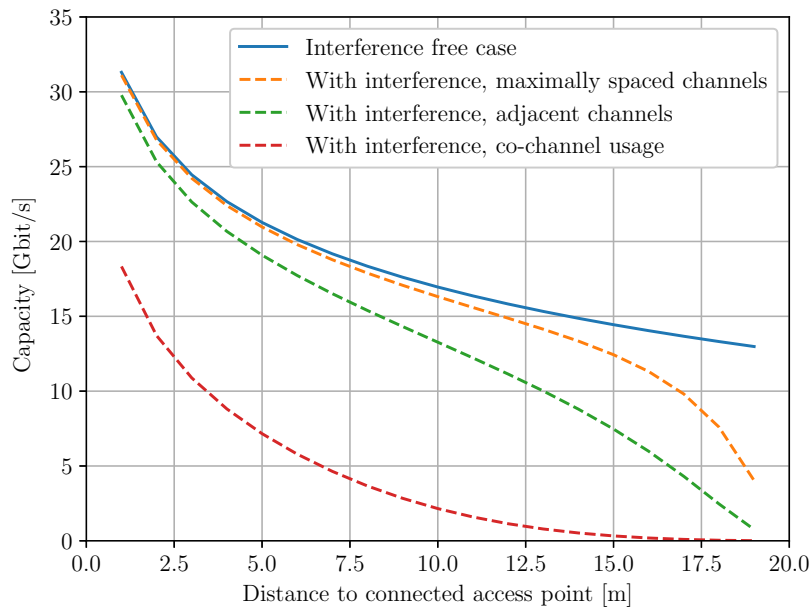


Figure 4.4: Capacity versus distance for four cases. Interference-free case, a case with adjacent channels (e.g. channels 1 and 2), maximally spaced channels (e.g. channel 1 and 4), and co-channel usage.

Table 4.1: Capacity performance degradation compared to interference free case for different channel usage. Based on results from interference study.

Configuration	Degradation at 5m	Degradation at 10m
Interference free	0 %	0 %
Far spaced channel usage	1 %	2 %
Adjacent band usage	6.7 %	25 %
Overlapping channel usage	67 %	85 %

gigabits per second, which in relative terms is not significant. If far away spaced channels are used (e.g. channel 1 and 4), then the interference effects are less noticeable. The interference effects are less noticeable for closer distances and get more significant at farther distances. When the same channel is used for both APs the performance is significantly reduced; however, the system is still functional. The idea is that a user in general should use the closest access point. If the middle of the carriage is considered, the adjacent channel usage would degrade the Shannon capacity by 25 %, and for the sparsely spaced channels only a degradation of a few percent is observed. If the same channel is used by the interfere, the performance is degraded by 85 %. The results are summarized in table 4.1. So, based on the simulation results, it can be concluded that it is possible to use this type of antenna installation with two access points per carriage in terms of interference, as long as they are operating on different channels.

4.2 Train measurement results

This section describes the results for the train measurements. Both TCP throughput and signal strength is covered, as well as the channel model.

4.2.1 Heatmap representation

The train carriage measurements show that it is feasible to use 60 GHz WLAN access points for train carriages with good performance (Gigabit speeds) and coverage. This can be seen in figures 4.5 and 4.6 showing heatmaps over signal strength (RSSI) and throughput. The receiver is specified to achieve MCS1 (385 Mbit/s) at -74 dBm received power. The heatmap figures were produced by using linear interpolation in logarithmic scale (e.g. linear in dB) between the recorded values. The active measurement area has a width of 2 meters and a length of about 16 meters. This covers the majority of the main interior area inside the train carriage. The train carriage had a width of 3 meters in total, hence the whole carriage was not used for active measurements due to tables being placed in the carriage.

In figure 4.5 it can be seen that the reported signal strength values are relatively stably decreasing with increased distance. The minimum signal strength value is about -68 dBm, and the highest value is -38 dBm. In figure 4.6 it can be seen that only a few "blind spots" with low throughput are found at distances of about 12 to

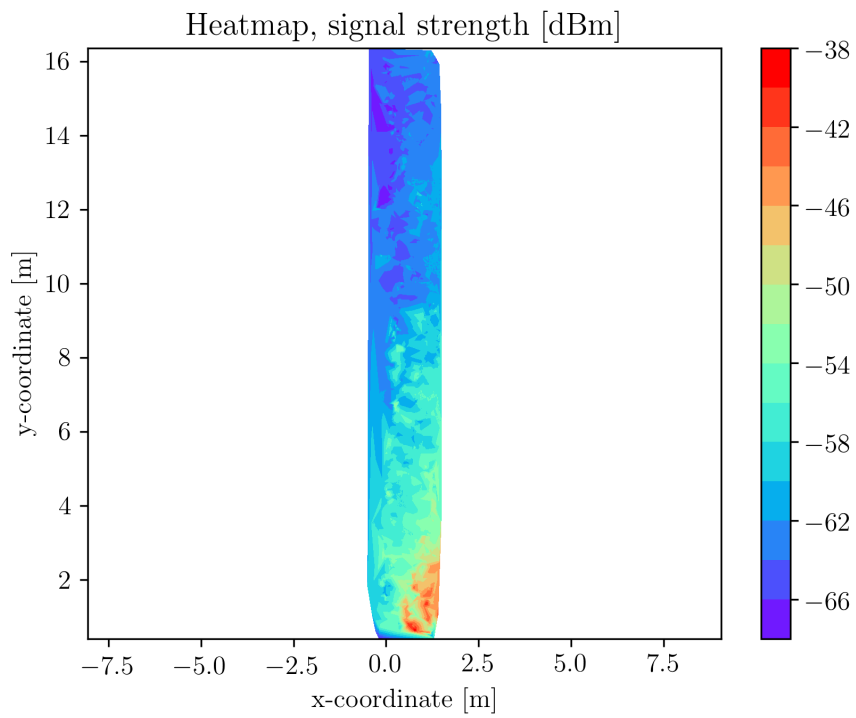


Figure 4.5: Heatmap of measured signal strength values.

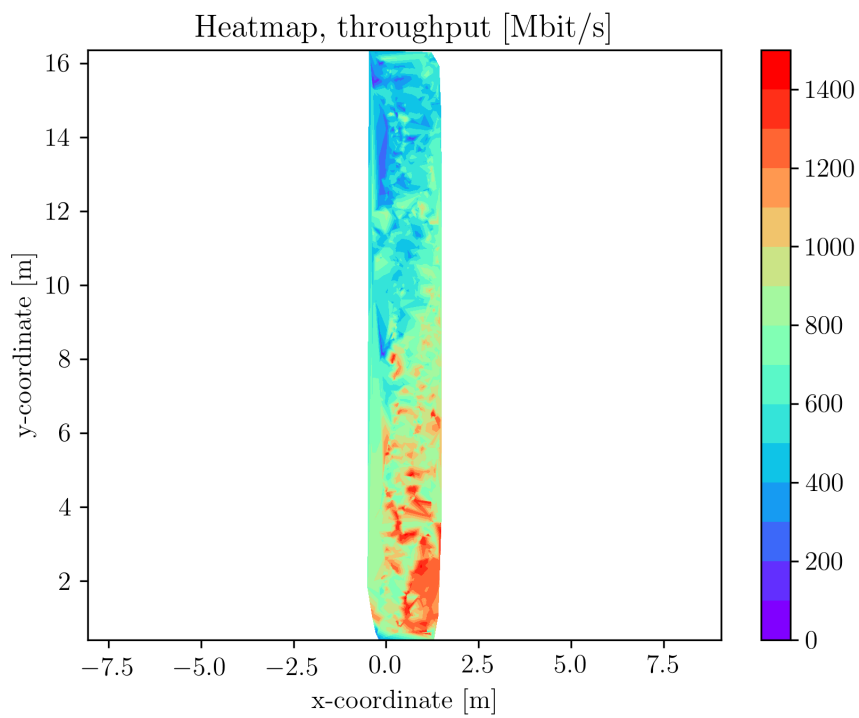


Figure 4.6: Heatmap of measured throughput values.

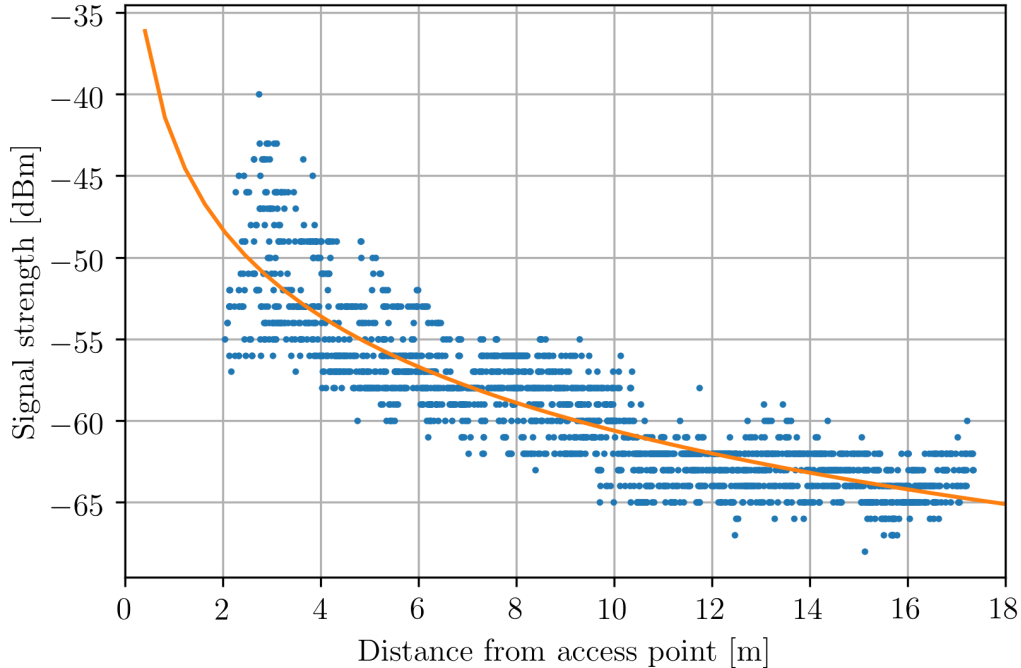


Figure 4.7: Signal strength versus distance from access point (blue). A regression line (orange) from the least-squares regression is shown for the modelled path loss.

Table 4.2: Measured path loss exponent, n , and standard deviation of the shadowing, σ_s for 60 GHz channel.

Scenario	Type	PL exponent, n	σ_s
Train carriage	LOS	1.50	2.17 dB

16 meters, this is most probably due to fading which at some positions is significant enough to reduce the throughput to close to zero. Except for these small blind spots at the end of the carriage, high throughputs can be seen for most of the carriage. There are several spots and areas where 1.4 Gbit/s is achieved.

4.2.2 Radio channel characterization results

In [43, Chapter 2], measured values of the pathloss exponent, n , range between 0.40 to 2.10 for LOS scenarios. For NLOS scenarios, n varied between 1.97 to 5.40. As presented in table 4.2, the path loss exponent measured in the train carriage is found to be 1.50. This is a reasonable value when comparing with other studies [43, Chapter 2] where path loss exponents for corridor environments varied from 0.87 to 2.29. Corridors can in some sense be considered as a comparable environment in terms of the geometrical shape, even though the actual materials, and hence reflection parameters, may differ. The shadowing standard deviation was found to be 2.17 dB which is also close to what is found in [43, Chapter 2] for similar environments such as offices. It is also of interest to study the distribution of the fading, X_σ . Although

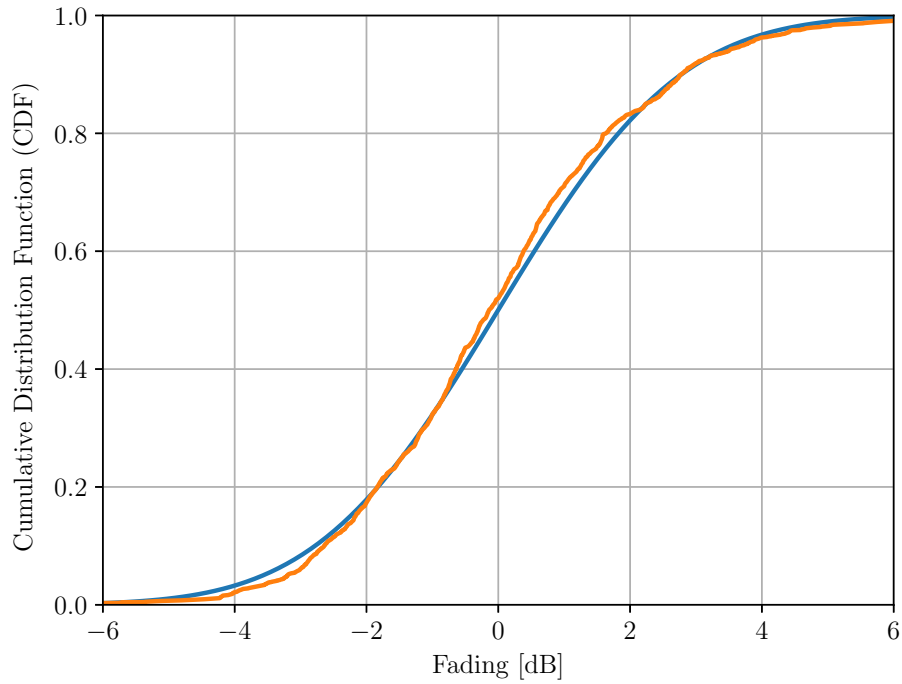


Figure 4.8: CDF of measured fading. Blue line is a fitted normal distribution, the orange is the empirical CDF.

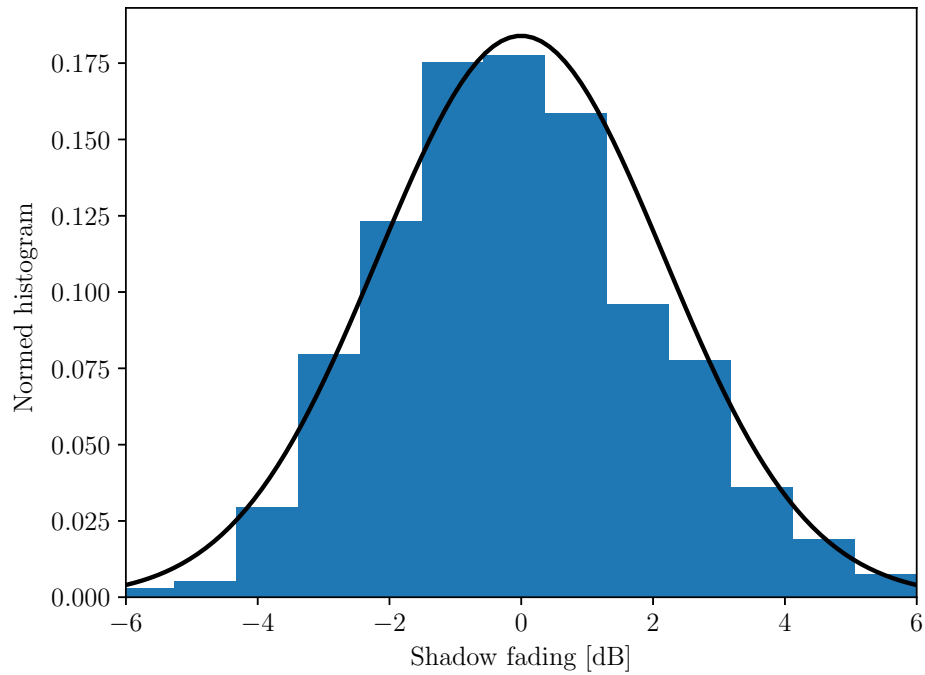


Figure 4.9: Histogram over the shadow fading, X_σ . Normalized so that the sum of all bars are equal to one.

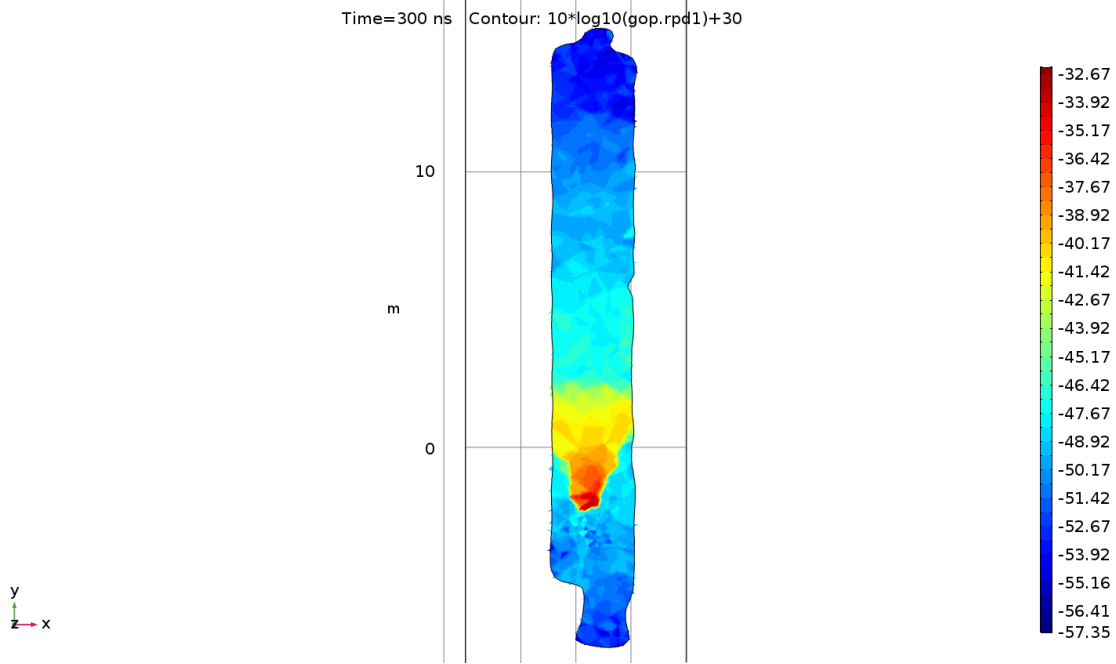


Figure 4.10: Heatmap of signal strength [dBm/m^2] from ray tracing simulations, based on the LIDAR scanned train carriage model. The results show the same characteristics as the measurements.

the parameter X_σ is denoted as shadow fading in the literature, this is not the case here since all the measurements are performed for LOS, hence no shadowing is experienced. Rather, X_σ represents fading due to multipath effects. The parameter is usually assumed to have a log-normal distribution, which has been verified in many studies [51]. The results agree with what previously have been found for 60 GHz indoor channel measurements in terms of the shadow fading distribution [52]. It can from Figure 4.8 be observed that the shadow fading has an approximately log-normal distribution. This is also verified by the histogram representation seen in Figure 4.9. Hence, the fading can be represented well by this type of distribution. This also indicates that the log-distance model very successfully models the channel.

4.3 Ray tracing results

A heatmap of the signal strength (based on the accumulated power of the incoming rays) is shown in figure 4.10. The train carriage has some small rooms, which explains the irregular shape seen in figure 4.10. As a comparison, a simplified geometry representing a train carriage was also used. It basically consisted of a cuboid with a table placed inside, with the same dimensions as the real train carriage. Figure 4.11 shows a heatmap of the signal strength based on ray tracing simulations for the simplified train carriage model. It can be seen that a similar kind of characteristics can be observed, as in the train carriage measurements. Consistent with the train carriage measurement results, it can be observed that the signal is strong in the first few meters, to later decay more significantly. The results of the ray

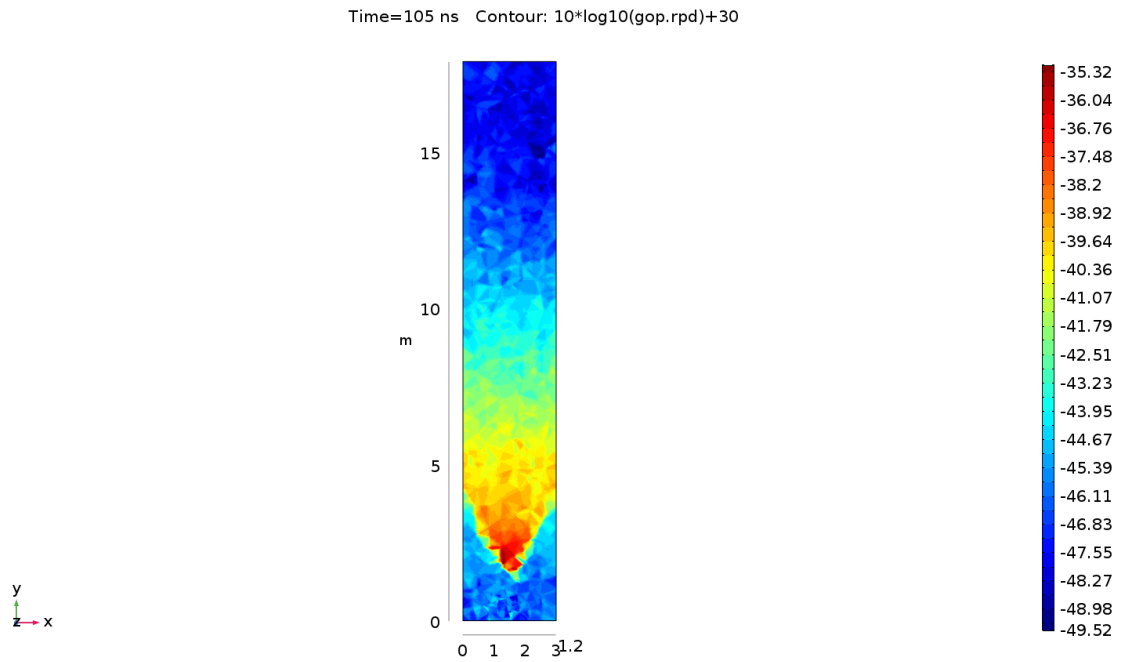


Figure 4.11: Heatmap of signal strength [dBm/m^3] from ray tracing simulations, based on the simplified train carriage model. The results show the same characteristics as the measurements.

tracing simulations are highly dependent on the 3D model used, as well as the assumed characteristics of the wall material. This was verified by comparing different variations and configurations.

4.4 Simulations and measurements comparison

The ray tracing simulations display the same characteristics as the measurements. However, the absolute values are not the same, this is most likely due to the fact that the ray tracing simulation setup does not correspond perfectly to the real scenario. However, the results are similar in relative terms, both the measurements and ray tracing simulations have a range of about 30 dB. It can also be due to that the ray tracing methods does not capture all the necessary propagation effects. The effects of the receive antenna are not directly captured by the ray tracing simulations, since the power accumulation is calculated per area, and hence the antennas radiation pattern should be taken into account for a more precise result.

5

Discussion

This chapter discusses the results and validity of each investigation method used. Measurement and model errors and their impact are discussed. The feasibility of 60 GHz access points for passenger Wi-Fi is discussed. Optimal antenna placement for such systems is discussed. Beamforming and spatial multiplexing implications of future systems is covered. 3GPP 5G is discussed, since millimeter waves will most likely be in use for some urban or indoor environments. In the end, a prediction about the future market adaptation of 802.11ad is performed.

5.1 Analytical method

It is important to remember that models containing some simplifications of reality were used for the capacity simulations. The performance in practice can differ due to effects of the 802.11 protocol. The effective throughput in real equipment is lower than channel capacity due to overhead and other non-idealities. The purpose behind the calculations is to provide a qualitative idea about the differences between these kinds of systems. The real outputs in a practical case would depend on all these system parameters, as well as the channel environment. The path loss model used here is only valid in LOS cases where there are no strong reflected waves being received. The path loss model and the assumed output powers and antenna gains can affect the results greatly due to the capacity function. If the receiver is operating in the linear region of the Shannon capacity function, it may be greatly affected by interference. However, for high values of SNR, the effects will be less noticeable. Hence, depending on the setup assumed, the amount of degradation due to interference may change.

Regarding the simulations trying to investigate the effects of interference, the idea of is not to provide an exact answer, but to provide insight on how interference can affect the system performance. The interference study is based on previous work [39]. The methodology used in this work is rather simple, and does not capture all the effects of the 802.11ad standard, and due to this, the results may differ from an empirical study. The results from the interference investigation were relatively close to what was found empirically in [10], especially for the ACI case. However the results are not directly comparable with the results in [10] due to differences in the setup.

The analytical method employs widely used models (link budget and standard mi-

crowave system engineering methods) and formulas, which are described in works such as [48, Chapter 14]. The uncertainty in the results relies on the validity of the assumptions made for the hardware and channel model. The channel model will most likely change depending on the deployment scenario, which will affect the results.

5.2 Train measurements

The path loss exponent was found to be 1.50 for the train carriage. This value is lower than the free space value of 2, meaning that the signal degrades slower than the free space case. The obtained path loss exponent is promising in terms of potential range, since the signal strength does not degrade significantly. The range of the system has twofold effects: a shorter range can yield more dense cells, however a longer range could reduce the number of access points needed. The measurement results are valid for this type of train carriage and under the certain measurement conditions. The results may change with different antenna types, access point and client placement heights, train interior, etc. However, this result is a scientific contribution and to the best of the author's knowledge there has been no channel characterization for 60 GHz in a train carriage previously published. The results from this measurement campaign are only applicable to this train carriage, and the results may not be directly transferable to other train carriage models. The layout inside the train is however similar to a lot of subway cars which have a more sparse interior, hence the measurements could be assumed to be approximately valid for this type of carriages.

There are a few error sources which need to be considered when analyzing the results. The position measurements have a location dependent measurement uncertainty. The location dependency is due to the increased uncertainty in the UWB positioning when the client has a large distance from the anchor points. The position has an estimated uncertainty of about 0.5 meters in the middle of the carriage, and of about 0.2 meters close to the edges of the carriage, when its close to one of the anchor points. The distance error will affect results when the signal strength and throughput is plotted against the distance. However, this error is estimated to have a minor impact. The radio equipment report the RSSI values, however it is up to every manufacturer exactly how to calculate this value. This manufacturer provides the RSSI values in integer values in dBm. It is assumed that the error of this value is less than 0.5 dB, based on that whole integer numbers are reported. When performing the radio measurements, there is a certain amount of antenna misalignment in the sense that the antennas are not always aimed perfectly at each other. Hence it can not for all positions be considered that the antennas main lobes are pointed precisely against each other. However, this is not a problem for a radio channel model, but it would distort the results for a propagation model.

5.3 Ray tracing simulations

The ray tracing simulations did display the same propagation characteristics as the measurements. However, for the characteristics to be similar, a very low reflection coefficient had to be used. If a higher coefficient was used, the radio power would degrade much more rapidly with increasing distance than what was measured. The absolute values of the signal strength were offset by a few decibels, this may be due to how the simulation was set up. The ray tracing results were highly dependent on what meshing was used for the 3D model. The reflection parameters also had a large impact on the final results.

The simulations does provide good insight on how the wall material and geometry of the train carriage affect the wave propagation. It also enables an easy way to try different access point placements. However, it is not trivial to map the results from the ray tracing to actual performance (e.g. throughput), since this will depend on the hardware used, and what assumptions are made about interference. It is also important to emphasize that ray tracing simulations are especially useful for millimeter wave simulations, compared to sub 6 GHz waves. This can in simple terms be explained by the fact that millimeter wave are more similar to optical rays compared to sub 6 GHz waves.

There are studies which have proven that ray tracing simulations can model an environment very well [44]. However, there are also examples of where ray tracing has failed to represent an environment. The final result is dependent on the assumed reflection parameters, which is something which was estimated. However, the results are in a sense validated by comparing with the experiments, which were performed in the same setup.

5.4 Feasibility of 60 GHz access points for passenger Wi-Fi

The radio measurements show that it is possible to cover an entire train carriage with only one 60 GHz access point. However, the measurement results are only valid for an empty train carriage. With passengers, the range of an access point is assumed to be reduced due to blockage and absorption. Based on this, a minimum of two access points per carriage is recommended, given the currently available technology. The capacity simulations also support this claim, and provide an upper bound of system performance. The reason that the measurements give lower throughputs than the capacity simulations is due to hardware and software constraints. The radio modules do not support such high rates, and the IEEE 802.11 standards has a significant overhead reducing the effective throughput.

There is an obvious trade off between number of access points, coverage and performance. Interference also comes into play, and due to the limited number of 60 GHz 802.11ad channels, interference will put an upper bound on the achievable perfor-

mance inside a train carriage. Even if high-gain ceiling-mounted antennas are used, the reflections may cause significant interference to other clients and access points. One key to partly resolve this issue would be to employ beamforming access points with a high number of elements, which could direct the energy only to the specific devices, reducing interference.

These results provide insight in how to build 802.11ad networks. Hence, the results contribute satisfying a need which has been identified by [10]. The results also break the common myth of 10 meter ranges of 60 GHz WLANs, based on the high throughput obtained inside the train carriage at distances up to 17 meters. This performance was achieved whilst still being well within the allowed power limits.

Using new 60 GHz systems could offload the 2.4 and 5 GHz bands, since some users will be served using the new 60 GHz band instead of current bands. This leads to yielding both a higher system throughput and a better user experience for all users, including those using devices without support of the new technology. This can be explained by that the throughput per user of a Wi-Fi access point will decrease with more connected users.

5.5 Optimal antenna placement

Based on the results obtained from measurements and simulations, it can be stated that it is possible to provide coverage with two access points for an empty train carriage. However, when humans are present, they will most likely act as absorbers, which will reduce the received power for any given client. Seating blockage will most likely play a significant part, and reduce the capacity for any given client. Human bodies will also act as blockage, as seen in [24], which will reduce the availability. By taking all this into consideration, it is recommended to use ceiling-mounted antennas rather than wall-mounted antennas. This is since less blockage can be expected by using ceiling-mounted antennas compared to wall-mounted antennas. By using relatively high-gain ceiling-mounted antennas, interference could potentially be reduced, as well as human blockage. Wall mounted antennas would also be viable, if it is not possible with a ceiling installation, but it would be more difficult to provide 100% coverage, due to human and seat blockage and absorption.

5.6 Beamforming implications

Beamforming is an important technique which will be an integral part of effective millimeter wave communication systems. It allows the antenna beam to be steered and shaped to direct energy to only where it is needed. This reduces interference, since more directive beams could be used, instead of more omni-directional antennas.

Already as of today beamforming is employed in many products [12][53], but the number of beamforming antenna elements is predicted to increase in the future, making it possible to have more narrow beams. In general there are less space

constraints for the antenna of an access point or access point, compared to a user terminal such as a smartphone. This will probably lead to that future systems have a larger antenna array at the access point side, and smaller ones at the user terminals. This fact is what the future massive MIMO systems are based on. This will yield very narrow beamwidths from the access point, but a bit more wide from the user terminals. It is important to mention beamforming since it will be such an integral part of future system designs. Current mainstream market 802.11ad chipsets support up to 32 antenna elements [53], however some state of the art cellular 5G products use 128 elements for receiving, and 128 elements for transmitting [54] and in some cases up to 512 antenna ports in TDD mode [54]. It can be expected that similar number of elements soon will be available for 802.11-based solutions.

5.7 Spatial multiplexing implications

Spatial multiplexing is a multi-antenna technique which allows for an increase in spectral efficiency. By using several antennas at both the transmitter and receiver sides, together with signal processing, it is possible to transmit multiple parallel streams over the same frequency and time resource, making more effective use of the radio spectrum. Spatial multiplexing is currently being used extensively in sub 6 GHz standards such as LTE and Wi-Fi, and is to some extent employed in some 802.11ad solutions. The implication which spatial multiplexing has to 60 GHz systems is that the performance can be greatly improved by using more antennas at each side. In terms of physics, 60 GHz systems are very suitable for spatial multiplexing. This is due to the small antenna sizes, combined with the fact that a relatively small spacing is required between the antennas due to the short wavelengths. The distance required by two antennas to experience a significantly different radio environment is proportional to the wavelength, which for a 60 GHz system is only about 5 mm. This is something which allows for communication system using spatial multiplexing to be much smaller for a 60 GHz system compared to a sub 6 GHz system, since less antenna spacing is required.

In the capacity calculation performed in Section 3.1.1 it is assumed that a single stream was used for simplicity, however it can be expected that future systems will use spatial multiplexing, which will increase the capacity. For example, by using a system with two transmit and two receive antennas, the capacity could be effectively doubled, given the right conditions.

5.8 3GPP 5G

When discussing millimeter wave communications it is important to mention the cellular standards as well as the WLAN standards. Several millimeter wave bands are being considered to be used in 5G standards in conjunction with sub 6 GHz bands. The frequency ranges vary per region, however in the United States frequency bands around 28 GHz, 37 GHz and 39 GHz are being considered [28]. The 60 GHz band have also been discussed for usage in 5G, but it does not seem to be

one of the first bands to be used in practice.

Cellular millimeter wave systems will most likely not be able to provide a good service directly to passengers inside public transportation vehicles in general, this is due to the high attenuation of the millimeter waves through the vehicles walls and windows. This prediction is supported by the high attenuation of millimeter waves for outdoor to indoor scenarios which has been observed in [55]. Penetration loss through different window types has been measured in [5] for up to 18 GHz. High attenuation is especially prominent in energy-saving windows [5] which most likely will be even more deployed in future public transportation vehicles. This motivates the usage of roof mounted antennas, and a system distributing the capacity inside the vehicle via access points. This will provide users with high capacity data service. By using Wi-Fi calling, a feature which is supported by a lot of operators, the users could also use the on board network for regular cellphone calls. Another way could be that the users are using sub 6 GHz cellular bands for cellphone calls, and use the on board Wi-Fi network for bandwidth intensive services such as streaming. Hence an on board WLAN millimeter wave communication system, as the one described, works in symbiosis with cellular millimeter wave systems, since the WLAN system can be seen as a type of relay. This will also free up resources in the cellular networks, since instead of passengers trying to communicate through the vehicle with poor connections, they will be provided high-capacity connection via the on board access points and router which connects to the roof-mounted antennas.

These speculations goes in line with what has been found by major organizations. Cisco predicts that for 5G networks in 2021, 48 % of end user data will be offloaded by Wi-Fi or small-cell networks [4].

5.9 Future market adaptation prediction

Qualcomms chipset Snapdragon 845 does have support for multi-gigabit 802.11ad [56]. The chipset is planned to be integrated in many flagship smartphones. However, it us up to the phone manufacturers whether or not they choose to support 802.11ad in the end or not. If the major market holders would implement 802.11ad, then this would very likely accelerate the whole 60 GHz market for consumer products. The 60 GHz market for point-to-point solutions have seen a lot of new products in only the last half year, with prices decreasing. 60 GHz point-to-point links offer the usage of unlicensed spectrum, and ease of installation, which in many cases makes it more competitive than wireless sub 6 GHz solutions or fibre solutions.

6

Conclusion

This chapter concludes the results and findings. First, the analytic simulation results are concluded, then the measurements, and finally the ray tracing simulations. An overall conclusion is given, and possible future work is described.

6.1 Analytic simulation results

The simulations show that 60 GHz access points are feasible for a train carriage scenario, given an empty train carriage. The capacity which is offered by a 60 GHz system is about tenfold higher than a 5 GHz system for short ranges, assuming no spatial multiplexing is used. The frequency planning will have a significant impact on the system performance due to interference from adjacent access points.

The effects of using the same, or closely spaced, WLAN channels inside a train carriage was investigated. The simulations indicate that co-channel usage is possible for the given simulation setup with wall mounted antennas, even though the performance is degraded. However, placing the antennas in the ceiling and pointing them towards the floor would be a more suitable configuration in terms of interference reduction.

6.2 Train measurements

The 60 GHz channel for the measured train carriage was characterized, and it was shown that the channel can successfully be modeled with the log-distance path loss model with log-normal fading. The channel was found to have a path loss exponent of 1.50, and a shadowing standard deviation of 2.17 dB. The values are similar to what have been measured in other works for office environments [43]. The fact that there is less signal degradation than free space ($n = 2$) can be explained by the fact that the waves are reflected on the floor, walls and ceiling. Hence it can be interpreted that the waves experience guided propagation [52]. The measurements show that it is possible to achieve gigabit-performance on board train coaches, with good coverage. Hence, it can be concluded that such installations of millimeter wave access points are feasible, taking regulatory aspects for indoor usage taken into account, for both the ETSI and FCC regions.

It is important to note that the actual performance in a future system will depend on both the access points and the client devices. Important performance limiting

factors include which transmit powers and antenna types will be used. It can be imagined that the radios in handheld devices may not be designed to transmit at the maximally allowed power level to reduce battery usage.

6.3 Ray tracing simulations

The radio propagation characteristics from the ray tracing simulations did coincide very well with the measurements, given that the wall reflectivity was set to obtain this. If the walls were set to absorb more power, then the characteristics did not coincide with the measurements.

6.4 Overall conclusion

Based on the measurements, simulations and theory review, it is shown that it is possible to provide gigabit-performance to a user inside a train carriage with 802.11ad based access points. It should be noted that this result has been obtained for this train carriage with one user and the possibility of generalizing of this result for all train carriage types and more number of passengers should be studied further. More RF absorption is expected when the number of passengers is increasing, resulting in weaker received signal strengths for user devices. Regarding system design recommendations, ceiling-mounted access points are recommended rather than wall mounted. This recommendation is based on optimally both in terms of interference and physical blockage.

6.5 Future work

Suitable future work could be performing similar measurements in a modern train carriage with original interior, in more user-like scenarios, such as a user being seated with a device in hand. It would also be interesting to vary the amount of passengers inside the carriage, and see how this affects the performance. Due to the rapid growth and advancement of the 60 GHz field, it would be of interest to try new equipment, for example 802.11ay devices, which might bring better performance and coverage due to MIMO, channel bonding and beamforming among other hardware and software improvements.

Regarding future simulations, as with the measurements, it would be of interest to investigate the effects of different numbers of users. More soft partitions such as seats and curtains could also be taken into account, to create a system level scenario more closely resembling a common train carriage in service with passengers. It would also be of interest to determine the optimal access point placement under those conditions, as well as the optimal number of access points. However, in practice, the number of access points is limited by available compartments and cost.

Bibliography

- [1] D. T. Fokum and V. S. Frost, “A survey on methods for broadband internet access on trains”, *IEEE Communications Surveys Tutorials*, vol. 12, no. 2, pp. 171–185, Second 2010, ISSN: 1553-877X. DOI: 10.1109/SURV.2010.021110.00060.
- [2] Z. Dong, P. L. Mokhtarian, G. Circella, and J. R. Allison, “The estimation of changes in rail ridership through an onboard survey: Did free Wi-Fi make a difference to Amtrak’s capitol corridor service?”, *Transportation*, vol. 42, no. 1, pp. 123–142, Jan. 2015, ISSN: 1572-9435. DOI: 10.1007/s11116-014-9532-7. [Online]. Available: <https://doi.org/10.1007/s11116-014-9532-7>.
- [3] Ericsson, *Ericsson Mobility Report 2017*, Ericsson, Ed., White paper, 2017. [Online]. Available: <https://www.ericsson.com/assets/local/mobility-report/documents/2017/ericsson-mobility-report-november-2017.pdf>.
- [4] *Cisco visual networking index: Global mobile data traffic forecast update, 2016–2021 white paper - Cisco*, <https://www.cisco.com/c/en/us/solutions/collateral/service-provider/visual-networking-index-vni/mobile-white-paper-c11-520862.html>, (Accessed on 04/11/2018),
- [5] P. Ängskog, M. Bäckström, and B. Vallhagen, “Measurement of radio signal propagation through window panes and energy saving windows”, in *2015 IEEE International Symposium on Electromagnetic Compatibility (EMC)*, Aug. 2015, pp. 74–79. DOI: 10.1109/ISEMC.2015.7256135.
- [6] J. Garcia, S. Alfredsson, A. Brunstrom, and C. Beckman, “Train velocity and data throughput - a large scale LTE cellular measurements study”, in *2017 IEEE 86th Vehicular Technology Conference (VTC-Fall)*, Sep. 2017, pp. 1–6. DOI: 10.1109/VTCFall.2017.8288294.
- [7] *FCC-13-112A1_Rcd.pdf*, https://apps.fcc.gov/edocs_public/attachmatch/FCC-13-112A1_Rcd.pdf, (Accessed on 02/12/2018),
- [8] *EN 302 567 - v1.2.1 - broadband radio access networks (BRAN); 60 GHz multiple-gigabit WAS/RLAN systems; harmonized EN covering the essential requirements of article 3.2 of the R&TTE directive*, <http://www.etsi>.

- org/deliver/etsi_en/302500_302599/302567/01_02_01_60/en_302567v010201p.pdf, (Accessed on 02/13/2018),
- [9] “ISO/IEC/IEEE international standard for information technology–telecommunications and information exchange between systems–local and metropolitan area networks–specific requirements–part 11: Wireless LAN medium access control (MAC) and physical layer (PHY) specifications amendment 3: Enhancements for very high throughput in the 60 GHz band (adoption of IEEE std 802.11ad-2012)”, *ISO/IEC/IEEE 8802-11:2012/Amd.3:2014(E)*, pp. 1–634, Mar. 2014. DOI: 10.1109/IEEESTD.2014.6774849.
- [10] K. Nguyen, M. G. Kibria, K. Ishizu, and F. Kojima, “Empirical investigation of IEEE 802.11ad network”, in *2017 IEEE International Conference on Communications Workshops (ICC Workshops)*, May 2017, pp. 192–197. DOI: 10.1109/ICCW.2017.7962656.
- [11] *Metrolinq™ 2.5g 60 PTP | IgniteNet*, <https://www.ignitenet.com/products/metrolinq-2-5-ptp/>, (Accessed on 02/12/2018),
- [12] *Gigaray modules & devices - Lattice Semiconductor*, <http://www.latticesemi.com/Products/mmWave/UltraGigBeamformingTX>, (Accessed on 02/12/2018),
- [13] *Nighthawk X10: The best WiFi router | 802.11ad | AD7200 (R9000) by NETGEAR*, <https://www.netgear.com/landings/ad7200/>, (Accessed on 02/26/2018),
- [14] *ZenFone 4 pro (ZS551KL, SE) | phone | ASUS Global*, <https://www.asus.com/Phone/ZenFone-4-Pro-ZS551KL-SE/>, (Accessed on 02/26/2018),
- [15] *Acer TravelMate P648-MG-789T*, <https://www.intel.com/content/www/us/en/products/devices-systems/laptops/notebooks/acer-travelmate-p648-mg-789t-h32303951.html>, (Accessed on 02/26/2018),
- [16] “IEEE standard for information technology–telecommunications and information exchange between systems–local and metropolitan area networks–specific requirements–part 11: Wireless LAN medium access control (MAC) and physical layer (PHY) specifications–amendment 4: Enhancements for very high throughput for operation in bands below 6 GHz.”, *IEEE Std 802.11ac(TM)-2013 (Amendment to IEEE Std 802.11-2012, as amended by IEEE Std 802.11ae-2012, IEEE Std 802.11aa-2012, and IEEE Std 802.11ad-2012)*, pp. 1–425, Dec. 2013. DOI: 10.1109/IEEESTD.2013.7797535.
- [17] K.-C. Huang and Z. Wang, *Millimeter wave communication systems*. Hoboken, N.J: Wiley, 2011, ISBN: 0470404620;9780470404621;

-
- [18] K.-C. Huang and D. J. Edwards, “Gigabit wireless communications”, in *Millimetre Wave Antennas for Gigabit Wireless Communications: A Practical Guide to Design and Analysis in a System Context*. Wiley Telecom, 2008, pp. 286–, ISBN: 9780470712467. DOI: 10.1002/9780470712467.ch1.
- [19] R. C. Daniels and R. W. Heath, “60 GHz wireless communications: Emerging requirements and design recommendations”, *IEEE Vehicular Technology Magazine*, vol. 2, no. 3, pp. 41–50, Sep. 2007, ISSN: 1556-6072. DOI: 10.1109/MVT.2008.915320.
- [20] M. Kinoshita, T. Hikage, T. Nojima, S. Futatsumori, A. Kohmura, and N. Yonemoto, “Numerical estimation of RF propagation characteristics of cellular radio in an aircraft cabin”, Barton, A.C.T: Engineers Australia, 2011, ISBN: 9781457720345;1457720345;9780858259744;0858259745;
- [21] V. Ziegler, B. Schulte, J. Sabater, S. Bovelli, J. Kunisch, K. Maulwurf, M. Martinez-Vazquez, C. Oikonomopoulos-Zachos, S. Glisic, M. Ehrig, and E. Grass, “Broadband 57-64-GHz WLAN communication system integrated into an aircraft cabin”, *IEEE Transactions on Microwave Theory and Techniques*, vol. 60, no. 12, pp. 4209–4219, 2012.
- [22] A. Chandra, T. Mikulasek, J. Blumenstein, and A. Prokes, “60 GHz mmW channel measurements inside a bus”, in *2016 8th IFIP International Conference on New Technologies, Mobility and Security (NTMS)*, Nov. 2016, pp. 1–5. DOI: 10.1109/NTMS.2016.7792423.
- [23] T. Huang, “Feasibility study of IEEE 802.11ad for vehicle-to-x communication”, no: EX009/2016, Master’s thesis, Chalmers University of Technology, 2016. [Online]. Available: <http://publications.lib.chalmers.se/records/fulltext/232902/232902.pdf>.
- [24] S. Collonge, G. Zaharia, and G. E. Zein, “Influence of the human activity on wide-band characteristics of the 60 GHz indoor radio channel”, *IEEE Transactions on Wireless Communications*, vol. 3, no. 6, pp. 2396–2406, Nov. 2004, ISSN: 1536-1276. DOI: 10.1109/TWC.2004.837276.
- [25] F. Lu, S. Imata, N. Kamiya, N. Suzuki, and K. Takeuchi, “Propagation characteristics and deployment of millimeter wave communication in bullet train car”, in *IEEE International Conference on Ubiquitous Wireless Broadband (ICUWB), 2015*, IEEE, 2015, pp. 1–6.
- [26] F. Firyaguna, J. Kibilda, C. Galiotto, and N. Marchetti, “Coverage and spectral efficiency of indoor mmWave networks with ceiling-mounted access points”, in *GLOBECOM 2017 - 2017 IEEE Global Communications Conference*, Dec. 2017, pp. 1–7. DOI: 10.1109/GLOCOM.2017.8254623.

- [27] K. Venugopal, M. C. Valenti, and R. W. Heath, “Interference in finite-sized highly dense millimeter wave networks”, in *Information Theory and Applications Workshop (ITA), 2015*, IEEE, 2015, pp. 175–180.
- [28] FCC, *Fact sheet: Spectrum frontiers order to identify, open up vast amounts of new high-band spectrum for next generation (5G) wireless broadband (as adopted)*, https://apps.fcc.gov/edocs_public/attachmatch/DOC-340310A1.pdf, (Accessed on 02/23/2018), Jul. 2016.
- [29] D. Tse and P. Viswanath, *Fundamentals of Wireless Communication*. Cambridge University Press, 2005. DOI: 10.1017/CB09780511807213.
- [30] C. R. Anderson and T. S. Rappaport, “In-building wideband partition loss measurements at 2.5 and 60 GHz”, *IEEE Transactions on Wireless Communications*, vol. 3, no. 3, pp. 922–928, May 2004, ISSN: 1536-1276. DOI: 10.1109/TWC.2004.826328.
- [31] R. Schertlen, T. Zwick, and W. Wiesbeck, “Characterization of car windows for transmission of millimetre-waves”, in *2000 30th European Microwave Conference*, Oct. 2000, pp. 1–4. DOI: 10.1109/EUMA.2000.338671.
- [32] A. Eitan, R. Zamir, and A. Sanderovich, *Reflection measurements at 60 GHz - IEEE 11-18/0401r0*, <https://mentor.ieee.org/802.11/dcn/18/11-18-0401-00-00ay-reflection-measurements.pptx>, (Accessed on 06/22/2018), 2018.
- [33] N. Moraitis and P. Constantinou, “Indoor channel measurements and characterization at 60 GHz for wireless local area network applications”, *IEEE Transactions on Antennas and Propagation*, vol. 52, no. 12, pp. 3180–3189, Dec. 2004, ISSN: 0018-926X. DOI: 10.1109/TAP.2004.836422.
- [34] *Wi-Fi CERTIFIED WiGig | Wi-Fi Alliance*, <https://www.wi-fi.org/discover-wi-fi/wi-fi-certified-wigig>, (Accessed on 04/11/2018),
- [35] T. Nitsche, C. Cordeiro, A. B. Flores, E. W. Knightly, E. Perahia, and J. C. Widmer, “IEEE 802.11ad: Directional 60 GHz communication for multi-gigabit-per-second wi-fi [invited paper]”, *IEEE Communications Magazine*, vol. 52, no. 12, pp. 132–141, Dec. 2014, ISSN: 0163-6804. DOI: 10.1109/MCOM.2014.6979964.
- [36] A. Maltsev *et al.*, *Channel models for IEEE 802.11ay, doc.: IEEE 802.11-15/1150r9*, <https://mentor.ieee.org/802.11/dcn/15/11-15-1150-09-00ay-channel-models-for-ieee-802-11ay.docx>, (Accessed on 06/22/2018), 2017.

-
- [37] *Www.ieee802.org/11/reports/tgay_update.htm*, http://www.ieee802.org/11/Reports/tgay_update.htm, (Accessed on 02/13/2018),
- [38] *Wi-Fi CERTIFIED WiGig: A new frontier for Wi-Fi*, https://www.wi-fi.org/download.php?file=/sites/default/files/private/wp_Wi-Fi_CERTIFIED_WiGig_20161024.pdf, (Accessed on 04/11/2018),
- [39] V. Angelakis, S. Papadakis, V. Siris, and A. Traganitis, “Adjacent channel interference in 802.11a: Modeling and testbed validation”, in *2008 IEEE Radio and Wireless Symposium*, Jan. 2008, pp. 591–594. DOI: 10.1109/RWS.2008.4463561.
- [40] L. Ahlin, J. Zander, and B. Slimane, *Principles of Wireless Communications*. Studentlitteratur AB, 2006, ISBN: 9144030800.
- [41] J. D. Matyjias, S. Kumar, and F. Hu, *Wireless network performance enhancement via directional antennas: models, protocols, and systems*. CRC Press, 2015.
- [42] C. Gustafson, “60 GHz wireless propagation channels: Characterization, modeling and evaluation”, PhD thesis, Lund University, 2014, ISBN: 978-91-7623-183-8. [Online]. Available: <http://portal.research.lu.se/portal/files/5361183/4810453.pdf>.
- [43] S. Yong, P. Xia, and A. Valdes-Garcia, *60 GHz technology for Gbps WLAN and WPAN: from theory to practice*. Chichester, West Sussex, U.K: Wiley, 2010, ISBN: 0470747706.
- [44] N. Sood, A. Ludwig, X. Zhang, F. Bouwman, P. Nowicki, C. Bantin, J. Siu, and C. D. Sarris, “Modeling and optimization of coverage in London underground subway tunnels”, in *2015 IEEE International Symposium on Antennas and Propagation USNC/URSI National Radio Science Meeting*, Jul. 2015, pp. 87–88. DOI: 10.1109/APS.2015.7304429.
- [45] A. Karstensen, W. Fan, I. Carton, and G. F. Pedersen, “Comparison of ray tracing simulations and channel measurements at mmWave bands for indoor scenarios”, European Association of Antennas and Propagation, 2016, pp. 1–5.
- [46] D. M. Pozar, *Microwave and RF Design of Wireless Systems*. Wiley, 2000, ISBN: 978-0-471-32282-5.
- [47] *COMSOL Multiphysics modeling software*, <https://www.comsol.se/>, (Accessed on 05/08/2018),
- [48] D. M. Pozar, *Microwave Engineering*. Wiley, 2011, ISBN: 978-0-470-63155-3.

- [49] *iPerf - the TCP, UDP and SCTP network bandwidth measurement tool*, <https://iperf.fr/>, (Accessed on 05/08/2018),
- [50] *Cloudcompare - open source project*, <http://www.cloudcompare.org/>, (Accessed on 05/08/2018),
- [51] K. Guan, B. Ai, Z. Zhong, C. F. López, L. Zhang, C. Briso-Rodríguez, A. Hrovat, B. Zhang, R. He, and T. Tang, “Measurements and analysis of large-scale fading characteristics in curved subway tunnels at 920 MHz, 2400 MHz, and 5705 MHz”, *IEEE Transactions on Intelligent Transportation Systems*, vol. 16, no. 5, pp. 2393–2405, Oct. 2015, ISSN: 1524-9050. DOI: 10.1109/TITS.2015.2404851.
- [52] M. Fryziel, C. Loyez, L. Clavier, N. Rolland, and P. A. Rolland, “Path-loss model of the 60 GHz indoor radio channel”, *Microwave and Optical Technology Letters*, vol. 34, no. 3, pp. 158–162, 2002.
- [53] *QCA9500 | Qualcomm*, <https://www.qualcomm.com/products/qca9500>, (Accessed on 02/26/2018),
- [54] *5G radio – Ericsson*, <https://www.ericsson.com/en/networks/offerings/5g/5g-radio>, (Accessed on 02/26/2018),
- [55] C. A. L. Diakhate, J. M. Conrat, J. C. Cousin, and A. Sibille, “Millimeter-wave outdoor-to-indoor channel measurements at 3, 10, 17 and 60 GHz”, in *2017 11th European Conference on Antennas and Propagation (EUCAP)*, Mar. 2017, pp. 1798–1802. DOI: 10.23919/EuCAP.2017.7928696.
- [56] *Snapdragon 845 mobile platform with Adreno 630 GPU and Hexagon 685 DSP | Qualcomm*, <https://www.qualcomm.com/products/snapdragon-845-mobile-platform>, (Accessed on 04/18/2018),
- [57] A. Maltsev *et al.*, *Channel models for 60 GHz WLAN systems - IEEE 802.11-09/0334r8*, <https://mentor.ieee.org/802.11/dcn/09/11-09-0334-08-00ad-channel-models-for-60-ghz-wlan-systems.doc>, (Accessed on 06/22/2018), 2010.

A

Appendix A

A.1 Measurement data

In this section the raw measurement data from the train carriage is presented. As described in earlier chapters, for each measurement series, the cart was placed nearby the station access point, and then moved slowly backwards until the end of the train carriage. The logging was then paused, and the cart was returned close to the station access point, and the procedure was repeated for six times in total, with a position shift each time to capture the whole available floor area.

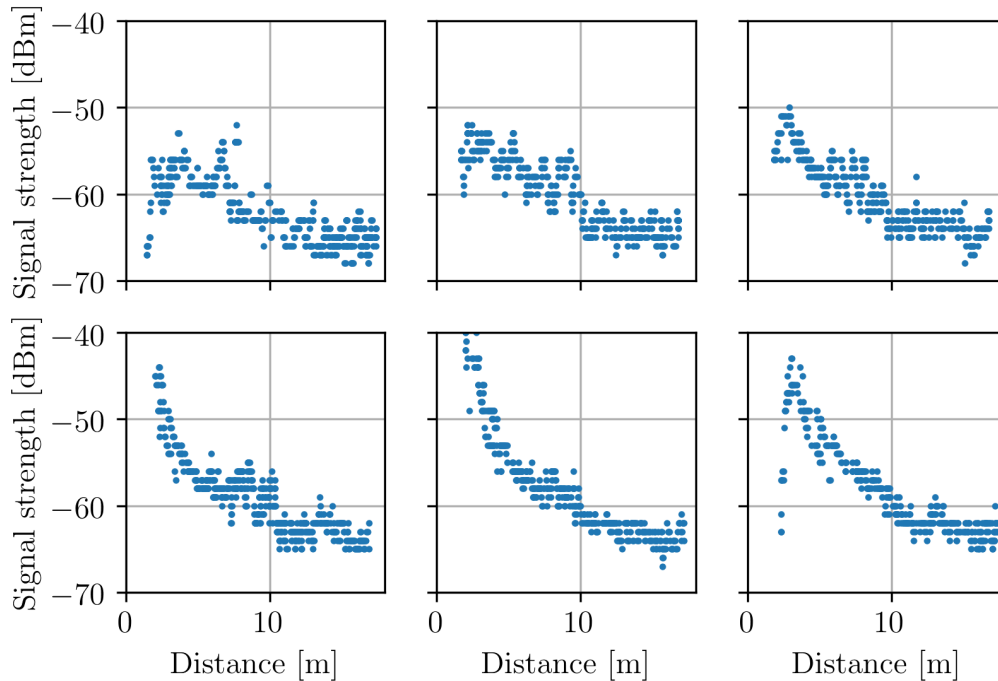


Figure A.1: Measured signal strength versus distance for the six runs used for the data analysis. From train carriage measurements.

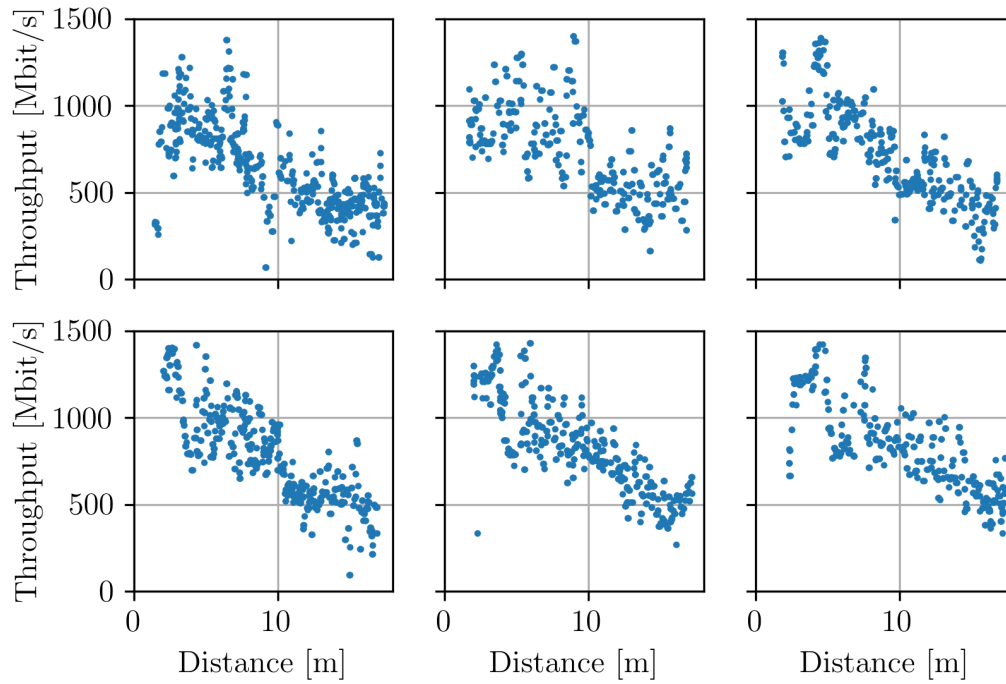


Figure A.2: Measured TCP throughput versus distance for the six runs used for the data analysis.. From train carriage measurements.

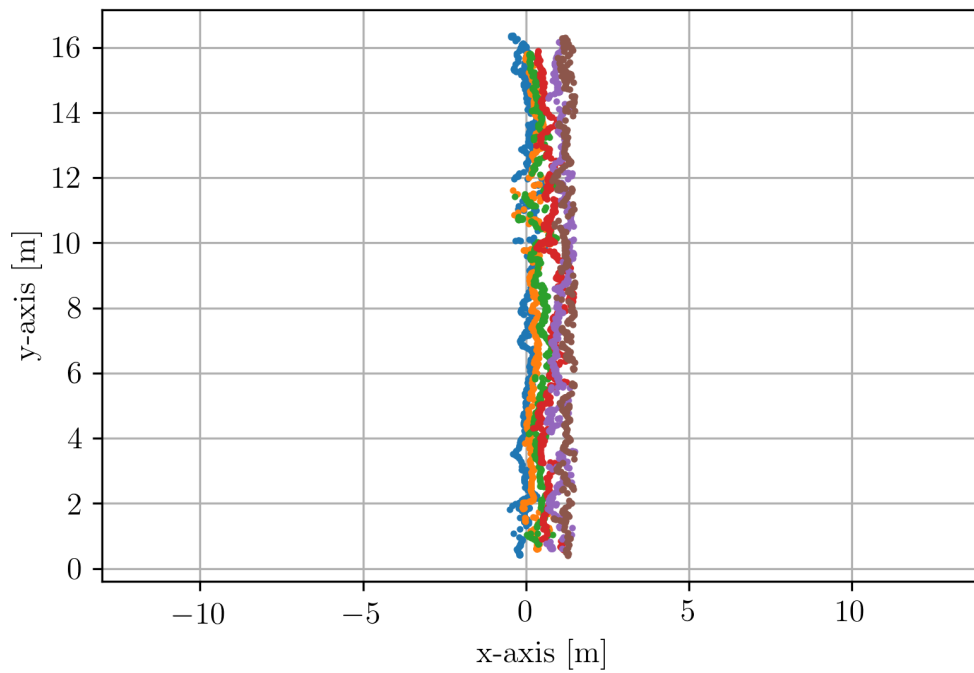


Figure A.3: Position measurements from UWB positioning system for train carriage measurements.

Table A.1: Summary of measurement series performed.

Environment	Date	Comment
Office	2018-02-03	Test and verification run
Office	2018-02-07	Test and verification run
Office	2018-02-10	System performed as intended
Train carriage	2018-02-12	Issues with positioning system
Train carriage	2018-02-14	Average accuracy of positioning measurements
Train carriage	2018-02-21	Highest accuracy of positioning measurements

A.2 Extended information about measurements

The measurements presented above are performed on the 21th of February, 2018. The temperature inside the train carriage was constantly held at 18 °C, and the outdoor temperature was approximately 0 °C. There are no known 60 GHz systems operating nearby that are suspected to have affected the measurements.

In table A.1 a complete appendix of all measurement series performed is presented. Only the set of measurements performed on the 21th of February is used for the analysis, since this campaign yielded the highest accuracy positioning measurements. The measurement series performed on the 14th of February yielded similar results as to the measurements performed on the 21th of February. Hence it can be considered that the measurements have been repeated due to that the same setup was used two times, and that similar results were obtained.

B

Appendix B

B.1 Antenna size for millimeter waves

For antennas which can be classified as aperture antennas such as reflector antennas, horn antennas, lens antennas and array antennas, the directivity, D , is given by [46, Chapter 4]

$$D = e_{ap} \frac{4\pi A}{\lambda^2} \quad (\text{B.1})$$

Where e_{ap} is the aperture efficiency, A is the physical aperture area, λ is the wavelength, which inversely proportional to the frequency. It can be seen that the directivity is proportional to the squared inverse of the wavelength, showing that a smaller wavelength yields higher directivity if the other parameters are constant. The antenna gain, G , is then given by [46, Chapter 4]

$$G = e_{rad} D \quad (\text{B.2})$$

Where e_{rad} is the radiation efficiency of the antenna. Hence for this type of systems significantly smaller antennas are required to achieve the same antenna gain for millimeter wave systems compared to sub 6 GHz systems, assuming that the factors such as aperture efficiency and radiation efficiency remains approximately the same.

C

Appendix C

C.1 Ray tracing computational times

For the reference of future works, the computational times for the ray tracing simulations are shown here. This gives an idea about the computational complexity. A modern ultrabook was used for the simulations, the specifications are shown in table C.2. The computational times are shown in C.1. To conclude, the ray tracing simulations are very rapid, given the complexity of the problem. If higher accuracy is required, more rays could be used. However, it seems that enough rays are used, since the results does not change significantly when the number of rays is increased. The mesh size is one of the parameters which mostly controls the computational time, this explains the difference in computational time between the LIDAR 3D model and the simple 3D model.

Table C.1: Summary of computational times.

Simulation	Time
Ray tracing, LIDAR 3D model	31 seconds
Ray tracing, simple 3D model	1 minute, 42 seconds

Table C.2: Specifications of PC used for simulations

Specifications	Type
CPU	Intel Core i7, I7-8550U
RAM	16 GB DDR4 SDRAM
GPU	Intel HD Graphics 620
HDD	256 GB SSD
OS	Ubuntu 16.04

D

Appendix D

D.1 More about channel modelling

An overview of channel modeling approaches [43] is shown in figure D.1.

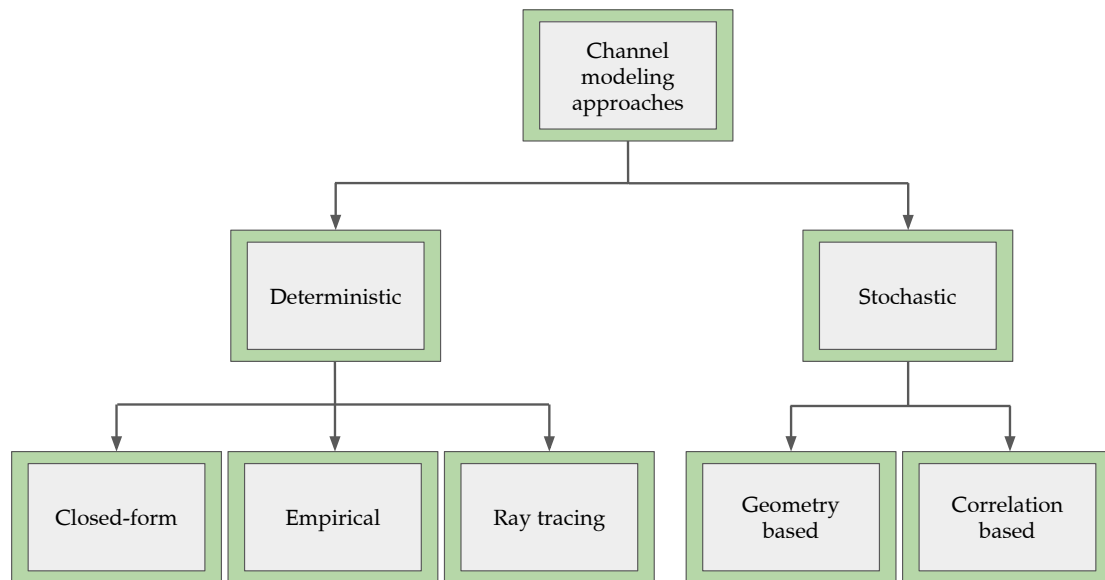


Figure D.1: Overview of channel modeling approaches [43].

Stochastic models are created from large amounts of measurement data to create a statistical representation of the channel [43]. In the geometry based stochastic models (GBSM), a group of scatterers are placed according to a specific statistical distribution, and the received signal is then calculated by superposition of all received scattered signals. Correlation-based models is popular in multi-antenna systems [43], is a method where the whole signal matrix is derived (e.g. by measurements), this allows for easy analysis of the multi-antenna performance. There is an official IEEE 802.11ad channel model specified in [57]. The model is based on the so called clustering approach. The 60 GHz propagation is often clustered which has been verified by several experiments [57], and the clusters can accurately be predicted by ray tracing methods [57].